International Tables for Crystallography (2006). Vol. C, Chapter 9.2, pp. 752–773.

9.2. Layer stacking

By S. Ďurovič, P. Krishna and D. Pandey

9.2.1. Layer stacking in close-packed structures (By D. Pandey and P. Krishna)

The crystal structures of a large number of materials can be described in terms of stacking of layers of atoms. This chapter provides a brief account of layer stacking in materials with structures based on the geometrical principle of close packing of equal spheres.

9.2.1.1. *Close packing of equal spheres*

9.2.1.1.1. *Close-packed layer*

In a close-packed layer of spheres, each sphere is in contact with six other spheres as shown in Fig. 9.2.1.1. This is the highest number of nearest neighbours for a layer of identical spheres and therefore yields the highest packing density. A single close-packed layer of spheres has two-, three- and sixfold axes of rotation normal to its plane. This is depicted in Fig. 9.2.1.2(*a*), where the size of the spheres is reduced for clarity. There are three symmetry planes with indices $(1\bar{2}.0)$, $(\bar{2}1.0)$, and (11.0) defined with respect to the smallest two-dimensional hexagonal unit cell shown in Fig. 9.2.1.2(*b*). The point-group symmetry of this layer is 6*mm* and it has a hexagonal lattice. As such, a layer with such an arrangement of spheres is often called a hexagonal close-packed layer. We shall designate the positions of spheres in the layer shown in Fig. 9.2.1.1 by the letter '*A*'. This *A* layer has two types of triangular interstices, one with the apex angle up (△) and the other with the apex angle down (▽). All interstices of one kind are related by the same hexagonal lattice as that for the *A* layer. Let the positions of layers with centres of spheres above the centres of the △ and ▽ interstices be designated as '*B*' and '*C*', respectively. In the cell of the *A* layer shown in Fig. 9.2.1.1 ($a = b =$ diameter of the sphere and $\gamma = 120°$), the three positions *A*, *B*, and *C* on projection have coordinates (0, 0), $(\frac{1}{3}, \frac{2}{3})$, and $(\frac{2}{3}, \frac{1}{3})$, respectively.

9.2.1.1.2. *Close-packed structures*

A three-dimensional close-packed structure results from stacking the hexagonal close-packed layers in the *A*, *B*, or *C* position with the restriction that no two successive layers are in identical positions. Thus, any sequence of the letters *A*, *B*, and *C*, with no two successive letters alike, represents a possible manner of stacking the hexagonal close-packed layers. There are thus infinite possibilities for close-packed layer stackings. The identity period *n* of these layer stackings is determined by the number of layers after which the stacking sequence starts repeating itself. Since there are two possible positions for a new layer on the top of the preceding layer, the total number of possible layer stackings with a repeat period of *n* is 2^{n-1}.

In all the close-packed layer stackings, each sphere is surrounded by 12 other spheres. However, it is touched by all 12 spheres only if the axial ratio h/a is $\sqrt{2/3}$, where *h* is the separation between two close-packed layers and *a* is the diameter of the spheres (Verma & Krishna, 1966). Deviations from the ideal value of the axial ratio are common, especially in hexagonal metals (Cottrell, 1967). The arrangement of spheres described above provides the highest packing density of 0.7405 in the ideal case for an infinite lattice (Azaroff, 1960). There are, however, other arrangements of a finite number of equal spheres that have a higher packing density (Boerdijk, 1952).

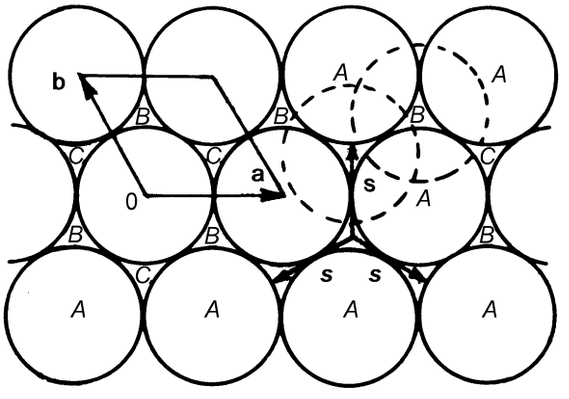

Fig. 9.2.1.1. The close packing of equal spheres in a plane.

9.2.1.1.3. *Notations for close-packed structures*

In the Ramsdell notation, close-packed structures are designated as *nX*, where *n* is the identity period and *X* stands for the lattice type, which, as shown later, can be hexagonal (*H*), rhombohedral (*R*), or in one special case cubic (*C*) (Ramsdell, 1947).

In the Zhdanov notation, use is made of the stacking offset vector **s** and its opposite −**s**, which cause, respectively, a

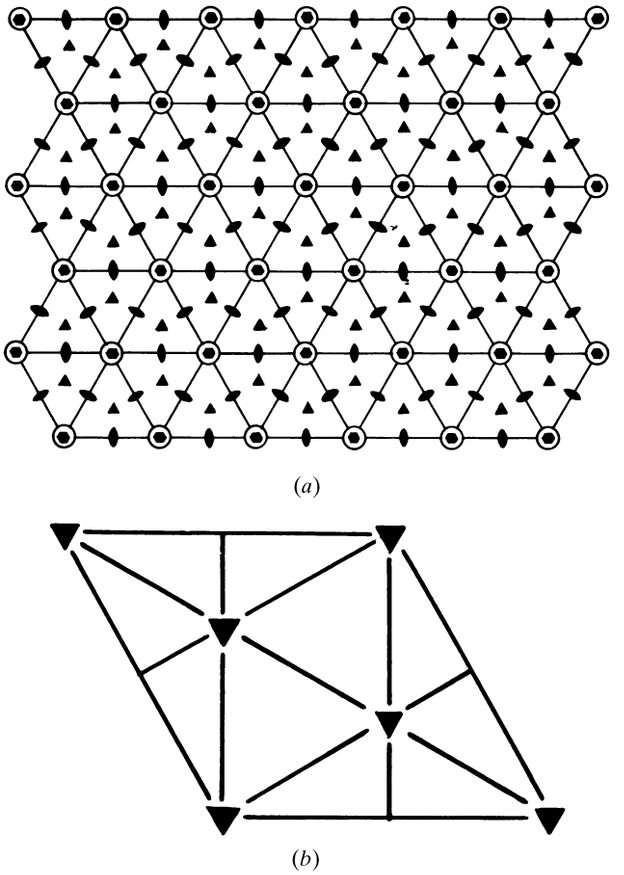

(*a*)

(*b*)

Fig. 9.2.1.2. (*a*) Symmetry axes of a single close-packed layer of spheres and (*b*) the minimum symmetry of a three-dimensional close packing of spheres.

Table 9.2.1.1. *Common close-packed metallic structures*

Stacking sequence	Identity period	Ramsdell notation	Zhdanov notation	Jagodzinski notation	Prototype
$AB, A\ldots$	2	2*H*	11	*h*	Mg
$ABC, A\ldots$	3	3*C*	∞	*c*	Cu
$ABCB, A\ldots$	4	4*H*	22	*hc*	La
$ABCBCACAB, A\ldots$	9	9*R*	21	*hhc*	Sm

cyclic ($A \rightarrow B \rightarrow C \rightarrow A$) or anticyclic ($A \rightarrow C \rightarrow B \rightarrow A$) shift of layers in the same plane. The vector **s** can be either (1/3)[$1\bar{1}00$], (1/3)[$01\bar{1}0$], or (1/3)[$\bar{1}010$]. Zhdanov (1945) suggested summing the number of consecutive offsets of each kind and designating them by numeral figures. Successive numbers in the Zhdanov symbol have opposite signs. The rhombohedral stackings have three identical sets of Zhdanov symbols in an identity period. It is usually sufficient to write only one set.

Yet another notation advanced, amongst others, by Jagodzinski (1949*a*) makes use of configurational symbols for each layer. A layer is designated by the symbol *h* or *c* according as its neighbouring layers are alike or different. Letter '*k*' in place of '*c*' is also used in the literature.

Some of the common close-packed structures observed in metals are listed in Table 9.2.1.1 in terms of all the notations.

9.2.1.2. *Structure of compounds based on close-packed layer stackings*

Frequently, the positions of one kind of atom or ion in inorganic compounds, such as SiC, ZnS, CdI_2, and GaSe, correspond approximately to those of equal spheres in a close packing, with the other atoms being distributed in the voids. All such structures will also be referred to as close-packed structures though they may not be ideally close packed. In the close-packed compounds, the size and coordination number of the smaller atom/ion may require that its close-packed neighbours in the neighbouring layers do not touch each other.

9.2.1.2.1. *Voids in close packing*

Three-dimensional close packings of spheres have two kinds of voids (Azaroff, 1960):

(i) If the triangular interstices in a close-packed layer have spheres directly over them, the resulting voids are called tetrahedral voids because the four spheres surrounding the void are arranged at the corners of a regular tetrahedron (Figs. 9.2.1.3*a*,*b*). If *R* denotes the radius of the four spheres surrounding a tetrahedral void, the radius of the sphere that would just fit into this void is given by 0.225*R* (Verma & Krishna, 1966). The centre of the tetrahedral void is located at a distance 3*h*/4 from the centre of the sphere on top of it.

(ii) If the triangular interstices pointing up in one close-packed layer are covered by triangular interstices pointing down in the adjacent layer, the resulting voids are called octahedral voids (Figs. 9.2.1.3*c*,*d*) since the six spheres surrounding each such void lie at the corners of a regular octahedron. The radius of the sphere that would just fit into an octahedral void is given by 0.414*R* (Verma & Krishna, 1966). The centre of this void is located half way between the two layers of spheres.

While there are twice as many tetrahedral voids as the spheres in close packing, the number of octahedral voids is equal to the number of spheres (Krishna & Pandey, 1981).

9.2.1.2.2. *Structures of SiC and ZnS*

SiC has a binary tetrahedral structure in which Si and C layers are stacked alternately, each carbon layer occupying half the tetrahedral voids between successive close-packed silicon layers. One can regard the structure as consisting of two identical interpenetrating close packings, one of Si and the other of C, with the latter displaced relative to the former along the stacking axis through one fourth of the layer spacing. Since the positions of C atoms are fixed relative to the positions of layers of Si atoms, it is customary to use the letters *A*, *B*, and *C* as representing Si–C double layers in the close packing. To be more exact, the three kinds of layers need to be written as $A\alpha$, $B\beta$, and $C\gamma$ where Roman and Greek letters denote the positions of Si and C atoms, respectively. Fig. 9.2.1.4 depicts the structure of SiC-6*H*, which is the most common modification.

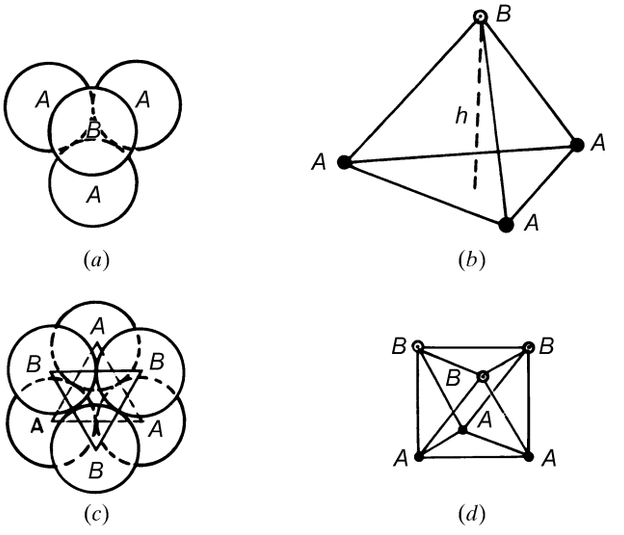

Fig. 9.2.1.3. Voids in a close packing: (*a*) tetrahedral void; (*b*) tetrahedron formed by the centres of spheres; (*c*) octahedral void; (*d*) octahedron formed by the centres of spheres.

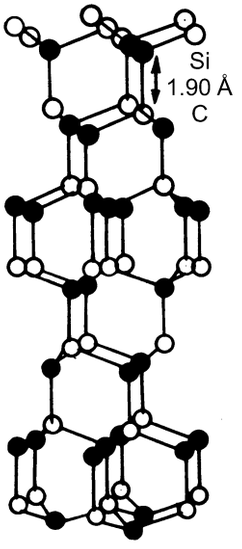

Fig. 9.2.1.4. Tetrahedral arrangement of Si and C atoms in the SiC-6*H* structure.

Table 9.2.1.2. *List of SiC polytypes with known structures in order of increasing periodicity (after Pandey & Krishna, 1982a)*

Polytype	Structure (Zhdanov sequence)	Polytype	Structure (Zhdanov sequence)
$2H$	11	$57H$	$(23)_9 3333$
$3C$	∞	$57R$	$(33)_2 34$
$4H$	22	$69R_1$	$(33)_3 32$
$6H$	33	$69R_2$	33322334
$8H$	44	$75R_2$	$(32)_3(23)_2$
$10H$	3322	$81H$	$(33)_5 35(33)_6 34$
$14H$	$(22)_2 33$	$84R$	$(33)_3(32)_2$
$15R$	23	$87R$	$(33)_4 32$
$16H_1$	$(33)_2 22$	$90R$	$(23)_4 3322$
$18H$	$(22)_3 33$	$93R$	$(33)_4 34$
$19H$	$(23)_3 22$	$96R_1$	$(33)_3 3434$
$20H$	$(22)_3 44$	$99R$	$(33)_4 3222$
$21H$	333534	$105R$	$(33)_5 32$
$21H_2$	$(33)_2 63$	$111R$	$(33)_5 34$
$21R$	34	$120R$	$(22)_5 23222333$
$24R$	35	$123R$	$(33)_6 32$
$27H$	$(33)_2(23)_3$	$126R$	$(33)_2 2353433223$
$27R$	2223	$129R$	$(33)_6 34$
$33R$	3332	$125R$	$32(33)_2 23(33)_3 23$
$33H$	$(33)_2 353334$	$141R$	$(33)_7 32$
$34H$	$(33)_4 2332$	$147R$	$(3332)_4 32$
$36H_1$	$(33)_2 32(33)_2 34$	$150R_1$	$(23)_3 32(23)_3 322332$
$36H_2$	$(33)_4 3234$	$150R_2$	$(23)_2(3223)_4$
$39H$	$(33)_2 32(33)_3(32)_2$	$159R$	$(33)_8 32$
$39R$	3334	$168R$	$(23)_{10} 33$
$40H$	$(33)_5 2332$	$174R$	$(33)_6 6(33)_5 4$
$45R$	$(23)_2 32$	$189R$	$(34)_8 43$
$51R_1$	$(33)_2 32$	$267R$	$(23)_{17} 22$
$51R_2$	$(22)_3 23$	$273R$	$(23)_{17} 33$
$54H$	$(33)_6 323334$	$393R$	$(33)_{21} 32$

A large number of crystallographically different modifications of SiC, called polytypes, has been discovered in commercial crystals grown above 2273 K (Verma & Krishna, 1966; Pandey & Krishna, 1982*a*). Table 9.2.1.2 lists those polytypes whose structures have been worked out. All these polytypes have $a = b = 3.078$ Å and $c = n \times 2.518$ Å, where n is the number of Si–C double layers in the hexagonal cell. The $3C$ and $2H$ modifications, which normally result below 2273 K, are known to undergo solid-state structural transformation to $6H$ (Jagodzinski, 1972; Krishna & Marshall, 1971*a*,*b*) through a non-random insertion of stacking faults (Pandey, Lele & Krishna, 1980*a*,*b*,*c*; Kabra, Pandey & Lele, 1986). The lattice parameters and the average thickness of the Si–C double layers vary slightly with the structure, as is evident from the h/a ratios of 0.8205 (Adamsky & Merz, 1959), 0.8179, and 0.8165 (Taylor & Jones, 1960) for the $2H$, $6H$, and $3C$ structures, respectively. Even in the same structure, crystal-structure refinement has revealed variation in the thickness of Si–C double layers depending on their environment (de Mesquita, 1967).

The structure of ZnS is analogous to that of SiC. Like the latter, ZnS crystals grown from the vapour phase also display a large variety of polytype structures (Steinberger, 1983). ZnS crystals that occur as minerals usually correspond to the wurtzite ($/AB/\ldots$) and the sphalerite ($/ABC/\ldots$) modifications. The structural transformation between the $2H$ and $3C$ structures of ZnS is known to be martensitic in nature (Sebastian, Pandey & Krishna, 1982; Pandey & Lele, 1986*b*). The h/a ratio for ZnS-$2H$ is 0.818, which is somewhat different from the ideal value (Verma & Krishna, 1966). The structure of the stackings in polytypic AgI is analogous to those in SiC and ZnS (Prager, 1983).

9.2.1.2.3. *Structure of CdI_2*

The structure of cadmium iodide consists of a close packing of the I ions with the Cd ions distributed amongst half the octahedral voids. Thus, the Cd and I layers are not stacked alternately; there is one Cd layer after every two I layers as shown in Fig. 9.2.1.5. The structure actually consists of molecular sheets (called minimal sandwiches) with a layer of Cd ions sandwiched between two close-packed layers of I ions. The bonding within the minimal sandwich is ionic in character and is much stronger than the bonding between successive sandwiches, which is of van der Waals type. The importance of polarization energy for the stability of such structures has recently been emphasized by Bertaut (1978). It is because of the weak van der Waals bonding between the successive minimal sandwiches that the material possesses the easy cleavage characteristic of a layer structure. In describing the layer stackings in the CdI_2 structure, it is customary to use Roman letters to denote the I positions and Greek letters for the Cd positions. The two most common modifications of CdI_2 are $4H$ and $2H$ with layer stackings $A\gamma B\,C\alpha B\ldots$ and $A\gamma B\,A\gamma B$, respectively. In addition, this material also displays a number of polytype modifications of large repeat periods (Trigunayat & Verma, 1976; Pandey & Krishna, 1982*a*). From the structure of CdI_2, it follows that the identity period of all such modifications must consist of an even number of I layers. The h/a ratio in all these modifications of CdI_2 is 0.805, which is very different from the ideal value (Verma & Krishna, 1966). The structure of PbI_2, which also displays a large number of polytypes, is analogous to CdI_2 with one important difference. Here, the distances between two I layers with and without an intervening Pb layer are quite different (Trigunayat & Verma, 1976).

9.2.1.2.4. *Structure of GaSe*

The crystal structure of GaSe consists of four-layered slabs, each of which contains two close-packed layers of Ga (denoted by symbols A, B, C) and Se (denoted by symbols α, β, γ) each in the sequence Se–Ga–Ga–Se (Terhell, 1983). The Se atoms sit on the corners of a trigonal prism while each Ga atom is tetrahedrally coordinated by three Se and one Ga atoms. If the Se layers are of A type, then the stacking sequence of the four

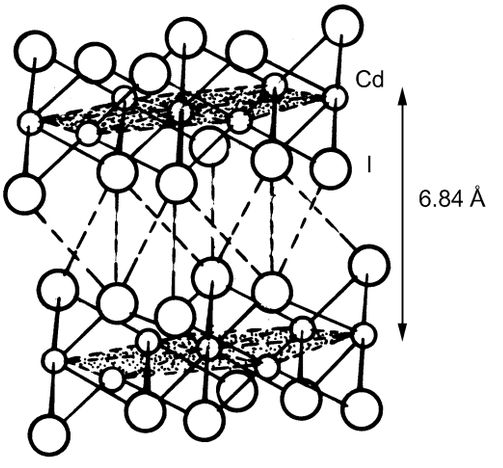

Fig. 9.2.1.5. The layer structure of CdI_2: small circles represent Cd ions and larger ones I ions (after Wells, 1945).

layers in the slab can be written as $A\beta\beta A$ or $A\gamma\gamma A$. There are thus six possible sequences for the unit slab. These unit slabs can be stacked in the manner described for equal spheres. Thus, for example, the $2H$ structure can have three different layer stackings: $/A\beta\beta A\,B\gamma\gamma B/\ldots$, $/A\beta\beta A\,B\alpha\alpha B/\ldots$ and $/A\beta\beta A\,C\beta\beta C/$. Periodicities containing up to 21 unit slabs have been reported for GaSe (see Terhell, 1983). The bonding between the layers of a slab is predominantly covalent while that between two adjacent slabs is of the van der Waals type, which imparts cleavage characteristics to this material.

9.2.1.3. *Symmetry of close-packed layer stackings of equal spheres*

It can be seen from Fig. 9.2.1.2(*a*) that a stacking of two or more layers in the close-packed manner still possesses all three symmetry planes but the twofold axes disappear while the sixfold axes coincide with the threefold axes (Verma & Krishna, 1966). The lowest symmetry of a completely arbitrary periodic stacking sequence of close-packed layers is shown in Fig. 9.2.1.2(*b*). Structures resulting from such stackings therefore belong to the trigonal system. Even though a pure sixfold axis of rotation is not possible, close-packed structures belonging to the hexagonal system can result by virtue of at least one of the three symmetry axes parallel to [00.1] being a 6_3 axis (Verma & Krishna, 1966). This is possible if the layers in the unit cell are stacked in special ways. For example, a $6H$ stacking sequence $/ABCACB/\ldots$ has a 6_3 axis through 0, 0. It follows that, for an nH structure belonging to the hexagonal system, n must be even. A packing nH/nR with n odd will therefore necessarily belong to the trigonal system and can have either a hexagonal or a rhombohedral lattice (Verma & Krishna, 1966).

Other symmetries that can arise by restricting the arbitrariness of the stacking sequence in the identity period are: (i) a centre of symmetry at the centre of either the spheres or the octahedral voids; and (ii) a mirror plane perpendicular to [00.1]. Since there must be two centres of symmetry in the unit cell, the centrosymmetric arrangements may possess both centres either at sphere centres/octahedral void centres or one centre each at the centres of spheres and octahedral voids (Patterson & Kasper, 1959).

9.2.1.4. *Possible lattice types*

Close packings of equal spheres can belong to the trigonal, hexagonal, or cubic crystal systems. Structures belonging to the hexagonal system necessarily have a hexagonal lattice, *i.e.* a lattice in which we can choose a primitive unit cell with $a = b \neq c$, $\alpha = \beta = 90^\circ$, and $\gamma = 120^\circ$. In the primitive unit cell of the hexagonal close-packed structure $/AB/\ldots$ shown in Fig. 9.2.1.6, there are two spheres associated with each lattice point, one at 0, 0, 0 and the other at $\frac{1}{3}, \frac{2}{3}, \frac{1}{2}$. Structures belonging to the trigonal system can have either a hexagonal or a rhombohedral lattice. By a rhombohedral lattice is meant a lattice in which we can choose a primitive unit cell with $a = b = c$, $\alpha = \beta = \gamma \neq 90^\circ$. Both types of lattice can be referred to either hexagonal or rhombohedral axes, the unit cell being non-primitive when a hexagonal lattice is referred to rhombohedral axes and *vice versa* (Buerger, 1953). In close-packed structures, it is generally convenient to refer both hexagonal and rhombohedral lattices to hexagonal axes. Fig. 9.2.1.7 shows a rhombohedral lattice in which the primitive cell is defined by the rhombohedral axes a_1, a_2, a_3; but a non-primitive hexagonal unit cell can be chosen by adopting the axes A_1, A_2, C. The latter has lattice points at $0, 0, 0$; $\frac{2}{3}, \frac{1}{3}, \frac{1}{3}$; and $\frac{1}{3}, \frac{2}{3}, \frac{2}{3}$. If this rhombohedral lattice is rotated through 60° around [00.1], the hexagonal unit cell will then be centred at $\frac{1}{3}, \frac{2}{3}, \frac{1}{3}$ and $\frac{2}{3}, \frac{1}{3}, \frac{2}{3}$. These two settings are crystallographically equivalent for close packing of equal spheres. They represent twin arrangements when both occur in the same crystal. The hexagonal unit cell of an nR structure is made up of three elementary stacking sequences of $n/3$ layers that are related to each other either by an anticyclic shift of layers $A \rightarrow C \rightarrow B \rightarrow A$ (obverse setting) or by a cyclic shift of layers $A \rightarrow B \rightarrow C \rightarrow A$ (reverse setting) in the direction of z increasing (Verma & Krishna, 1966). Evidently, n must be a multiple of 3 for nR structures.

In the special case of the close packing $/ABC/\ldots$ [with the ideal axial ratio of $\sqrt{(2/3)}$], the primitive rhombohedral unit cell has $\alpha = \beta = \gamma = 60^\circ$, which enhances the symmetry and enables the choice of a face-centred cubic unit cell. The relationship between the face-centred cubic and the rhombohedral unit cell is shown in Fig. 9.2.1.8. The threefold axis of the rhombohedral unit cell coincides with one of the ⟨111⟩ directions of the cubic unit cell. The close-packed layers are thus parallel to the {111} planes in the cubic close packing.

9.2.1.5. *Possible space groups*

It was shown by Belov (1947) that consistent combinations of the possible symmetry elements in close packing of equal spheres can give rise to eight possible space groups: $P3m1$, $P\bar{3}m1$,

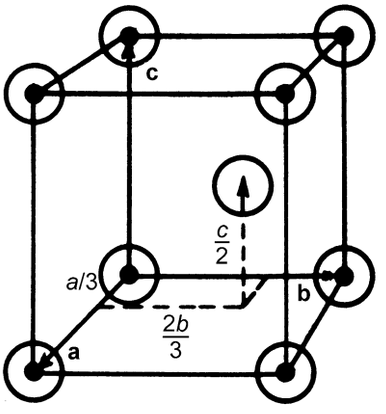

Fig. 9.2.1.6. The primitive unit cell of the $2H$ close packing.

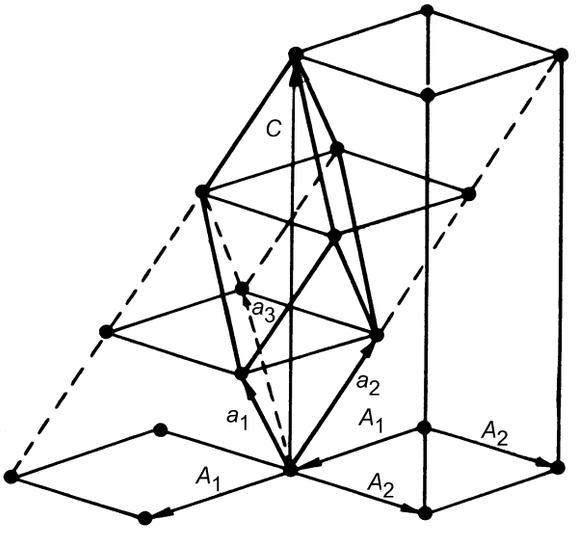

Fig. 9.2.1.7. A rhombohedral lattice (a_1, a_2, a_3) referred to hexagonal axes (A_1, A_2, C) (after Buerger, 1953).

$P\bar{6}m2$, $P6_3mc$, $P6_3/mmc$, $R3m$, $R\bar{3}m$, and $Fm3m$. The last space group corresponds to the special case of cubic close packing $/ABC/\ldots$. The tetrahedral arrangement of Si and C in SiC does not permit either a centre of symmetry ($\bar{1}$) or a plane of symmetry (m) perpendicular to [00.1]. SiC structures can therefore have only four possible space groups $P3m1$, $R3m1$, $P6_3mc$, and $F\bar{4}3m$. CdI_2 structures can have a centre of symmetry on octahedral voids, but cannot have a symmetry plane perpendicular to [00.1]. CdI_2 can therefore have five possible space groups: $P3m1$, $P\bar{3}m$, $R3m$, $R\bar{3}m$, and $P6_3mc$. Cubic symmetry is not possible in CdI_2 on account of the presence of Cd atoms, the sequence $/A\gamma BC\beta AB\alpha C/$ representing a 6R structure.

9.2.1.6. *Crystallographic uses of Zhdanov symbols*

From the Zhdanov symbols of a close-packed structure, it is possible to derive information about the symmetry and lattice type (Verma & Krishna, 1966). Let n_+ and n_- be the number of positive and negative numerals in the Zhdanov sequence of a given structure. The lattice is rhombohedral if $n_+ - n_- = \pm 1 \bmod 3$, otherwise it is hexagonal. The + sign corresponds to the reverse setting and − to the obverse setting of the rhombohedral lattice. Since this criterion is sufficient for the identification of a rhombohedral structure, the practice of writing three units of identical Zhdanov symbols has been abandoned in recent years (Pandey & Krishna, 1982*a*). Thus the 15R polytype of SiC is written as (23) rather than $(23)_3$.

As described in detail by Verma & Krishna (1966), if the Zhdanov symbol consists of an odd set of numbers repeated twice, *e.g.* (22), (33), (221221) *etc.*, the structure can be shown to possess a 6_3 axis. For the centre of symmetry at the centre of a sphere or an octahedral void, the Zhdanov symbol will consist of a symmetrical arrangement of numbers of like signs surrounding a single even or odd Zhdanov number, respectively. Thus, the structures (2)32(4)23 and (3)32(5)23 have centres of symmetry of the two types in the numbers within parentheses. For structures with a symmetry plane perpendicular to [00.1], the Zhdanov symbols consist of a symmetrical arrangement of a set of numbers of opposite signs about the space between two succession numbers. Thus, a stacking |522|225| has mirror planes at positions indicated by the vertical lines.

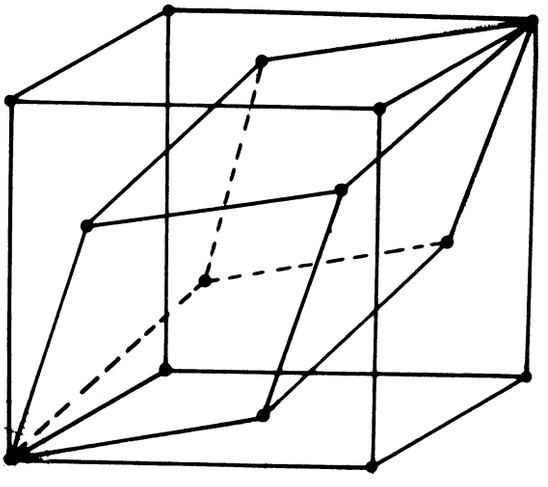

Fig. 9.2.1.8. The relationship between the f.c.c. and the primitive rhombohedral unit cell of the c.c.p. structure.

The use of abridged symbols to describe crystal structures has sometimes led to confusion in deciding the crystallographic equivalence of two polytype structures. For example, the structures (13) and (31) are identical for SiC but not for CdI_2 (Jain & Trigunayat, 1977*a*,*b*).

9.2.1.7. *Structure determination of close-packed layer stackings*

9.2.1.7.1. *General considerations*

The different layer stackings (polytypes) of the same material have identical a and b parameters of the direct lattice. The a^*b^* reciprocal-lattice net is therefore also the same and is shown in Fig. 9.2.1.9. The reciprocal lattices of these polytypes differ only along the c^* axis, which is perpendicular to the layers. It is evident from Fig. 9.2.1.9 that for each reciprocal-lattice row parallel to $\mathbf{c}^*$ there are five others with the same value of the radial coordinate ξ. For example, the rows 10.l, 01.l, $\bar{1}1.l$, $\bar{1}0.l$, $0\bar{1}.l$, and $1\bar{1}.l$ all have $\xi = |\mathbf{a}^*|$. Owing to symmetry considerations, it is sufficient to record any one of them on X-ray diffraction photographs. The reciprocal-lattice rows $hk.l$ can be classified into two categories according as $h - k = 0 \bmod 3$ or $\pm 1 \bmod 3$. Since the atoms in an nH or nR structure lie on three symmetry axes $A : [00.1]_{00}$, $B : [00.1]_{\frac{1}{3},-\frac{1}{3}}$, and $C : [00.1]_{-\frac{1}{3},\frac{1}{3}}$, the structure factor F_{hkl} can be split into three parts:

$$F_{hkl} = P + Q\exp[2\pi i(h-k)/3] + R\exp[-2\pi i(h-k)/3],$$

where $P = \sum_{z_A} \exp(2\pi i l z_A/n)$, $Q = \sum_{z_B} \exp(2\pi i l z_B/n)$, $R = \sum_{z_C} \exp(2\pi i l z_C/n)$, and z_A/n, z_B/n, z_C/n are the z coordinates of atoms at A, B, and C sites, respectively. For $h - k = 0 \bmod 3$,

$$F_{hkl} = P + Q + R = \sum_{z=0}^{n=-1} \exp(2\pi i l z/n),$$

which is zero except when $l = 0, n, 2n, \ldots$. Hence, the reflections 00.l, 11.l, 30.l, *etc.*, for which $h - k = 0 \bmod 3$, will be extinguished except when $l = 0, n, 2n, \ldots$. Thus, only those $hk.l$ reciprocal-lattice rows for which $h - k \neq 0 \bmod 3$ carry information about the stacking sequence and contain in general reflections with $l = 0, 1, 2, \ldots, n-1$, *etc.* It is sufficient to record any one such row, usually the 10.l row with $\xi = |\mathbf{a}^*|$, on an oscillation, Weissenberg, or precession photograph to obtain information about the lattice type, identity period, space group, and hence the complete structure (Verma & Krishna, 1966).

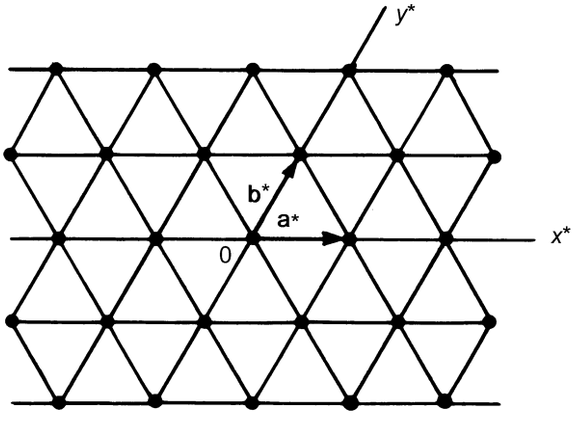

Fig. 9.2.1.9. The $\mathbf{a}^*$–$\mathbf{b}^*$ reciprocal-lattice net for close-packed layer stackings.

9.2.1.7.2. *Determination of the lattice type*

When the structure has a hexagonal lattice, the positions of spots are symmetrical about the zero layer line on the *c*-axis oscillation photograph. However, the intensities of the reflections on the two sides of the zero layer line are the same only if the structure possesses a 6_3 axis, and not for the trigonal system. An apparent mirror symmetry perpendicular to the *c* axis results from the combination of the 6_3 axis with the centre of symmetry introduced by X-ray diffraction. For a structure with a rhombohedral lattice, the positions of X-ray diffraction spots are not symmetrical about the zero layer line because the hexagonal unit cell is non-primitive causing the reflections *hkl* to be absent when $-h + k + l \neq 3n$ ($\pm n = 0, 1, 2, \ldots$). For the 10.*l* row, this means that the permitted reflections will have $l = 3n + 1$, which implies above the zero layer line $10.\bar{1}$, $10.\bar{4}$, $10.\bar{7}$, *etc*. reflections and below the zero layer line $10.\bar{2}$, $10.\bar{5}$, $10.\bar{8}$, *etc*. The zero layer line will therefore divide the distance between the nearest spots on either side (namely 10.1 and $10.\bar{2}$) approximately in the ratio 1:2. This enables a quick identification of a rhombohedral lattice. It is also possible to identify rhombohedral lattices by the appearance of an apparent 'doubling' of spots along the Bernal row lines on a rotation photograph. This is because of the threefold symmetry which makes reciprocal-lattice rows such as 10.*l*, $\bar{1}1.l$, and $01.\bar{l}$ identical with each other but different from the other identical set, 01.*l*, $\bar{1}0.l$, and $1\bar{1}.l$. The extinction condition for the second set requires $l = 3n - 1$, *i.e.* $l = 2, 5, 8$, and $\bar{1}, \bar{4}, \bar{7}$, *etc.*, which is different from that for the first set. Consequently, on the rotation photograph, reciprocal-lattice rows with $\xi = |\mathbf{a}^*|$ will have spots for $l = 3n \pm 1$ causing the apparent 'doubling'.

In crystals of layer structures, such as CdI_2, where *a*-axis oscillation photographs are normally taken, the identification of the rhombohedral lattice is performed by checking for the non-coincidence of the diffraction spots with those for the 2*H* or 4*H* structures. In an alternative method, one compares the positions of spots in two rows of the type 10.*l* and 20.*l*. This can conveniently be done by taking a Weissenberg photograph (Chadha, 1977).

9.2.1.7.3. *Determination of the identity period*

The number of layers, *n*, in the hexagonal unit cell can be found by determining the *c* parameter from the *c*-axis rotation or oscillation photographs and dividing this by the layer spacing *h* for that compound which can be found from reflections with $h - k = 0 \bmod 3$. The density of reciprocal-lattice points along rows parallel to $\mathbf{c}^*$ depends on the periodicity along the *c* axis. The larger the identity period along **c**, the more closely spaced are the diffraction spots along $\mathbf{c}^*$. In situations where there are not many structural extinctions, *n* can be determined by counting the number of spacings after which the sequence of relative intensities begins to repeat along the 10.*l* row of spots on an oscillation or Weissenberg photograph (Krishna & Verma, 1963). If the structure contains a random stacking disorder of close-packed layers (stacking faults), this will effectively make the **c** parameter infinite ($\mathbf{c}^* \rightarrow 0$) and lead to the production of characteristic continuous diffuse streaks along reciprocal-lattice rows parallel to $\mathbf{c}^*$ for reflections with $h - k \neq 0 \bmod 3$ (Wilson, 1942). It is therefore difficult to distinguish by X-ray diffraction between structures of very large unresolvable periodicities and those with random stacking faults. Lattice resolution in the electron microscope has been used in recent years to identify such structures (Dubey, Singh & Van Tendeloo, 1977). A better resolution of diffraction spots along the 10.*l* reciprocal-lattice row can be obtained by using the Laue method. Standard charts for rapid identification of SiC polytypes from Laue films are available in the literature (Mitchell, 1953). Identity periods as large as 594 layers have been resolved by this method (Honjo, Miyake & Tomita, 1950). Synchrotron radiation has been used for taking Laue photographs of ZnS polytypes (Steinberger, Bordas & Kalman, 1977).

9.2.1.7.4. *Determination of the stacking sequence of layers*

For an *nH* or 3*nR* polytype, the *n* close-packed layers in the unit cell can be stacked in 2^{n-1} possible ways, all of which cannot be considered for ultimate intensity calculations. A variety of considerations has therefore been used for restricting the number of trial structures. To begin with, symmetry and space-group considerations discussed in Subsection 9.2.1.4 and 9.2.1.5 can considerably reduce the number of trial structures.

When the short-period structures act as 'basic structures' for the generation of long-period polytypes, the number of trial structures is considerably reduced since the crystallographic unit cells of the latter will contain several units of the small-period structures with faults between or at the end of such units. The basic structure of an unknown polytype can be guessed by noting the intensities of 10.*l* reflections that are maximum near the positions corresponding to the basic structure. If the unknown polytype belongs to a well known structure series, such as $(33)_n32$ and $(33)_n34$ based on SiC-6*H*, empirical rules framed by Mitchell (1953) and Krishna & Verma (1962) can allow the direct identification of the layer-stacking sequence without elaborate intensity calculations.

It is possible to restrict the number of probable structures for an unknown polytype on the basis of the faulted matrix model of polytypism for the origin of polytype structures (for details see Pandey & Krishna, 1983). The most probable series of structures as predicted on the basis of this model for SiC contains the numbers 2, 3, 4, 5 and 6 in their Zhdanov sequence (Pandey & Krishna, 1975, 1976*a*). For CdI_2 and PbI_2 polytypes, the possible Zhdanov numbers are 1, 2 and 3 (Pandey & Krishna, 1983; Pandey, 1985). On the basis of the faulted matrix model, it is not only possible to restrict the numbers occurring in the Zhdanov sequence but also to restrict drastically the number of trial structures for a new polytype.

Structure determination of ZnS polytypes is more difficult since they are not based on any simple polytype and any number can appear in the Zhadanov sequence. It has been observed that the birefringence of polytype structures in ZnS varies linearly with the percentage hexagonality (Brafman & Steinberger, 1966), which in turn is related to the number of reversals in the stacking sequence, *i.e.* the number of numbers in the Zhdanov sequence. This drastically reduces the number of trial structures for ZnS (Brafman, Alexander & Steinberger, 1967).

Singh and his co-workers have successfully used lattice imaging in conjunction with X-ray diffraction for determining the structures of long-period polytypes of SiC that are not based on a simple basic structure. After recording X-ray diffraction patterns, single crystals of these polytypes were crushed to yield electron-beam-transparent flakes. The one- and two-dimensional lattice images were used to propose the possible structures for the polytypes. Usually this approach leads to a very few possibilities and the correct structure is easily determined by comparing the observed and calculated X-ray intensities for the proposed structures (Dubey & Singh, 1978; Rai, Singh, Dubey & Singh, 1986).

Direct methods for the structure determination of polytypes from X-ray data have also been suggested by several workers (Tokonami & Hosoya, 1965; Dornberger-Schiff & Farkas-

Jahnke, 1970; Farkas-Jahnke & Dornberger-Schiff, 1969) and have been reviewed by Farkas-Jahnke (1983). These have been used to derive the structures of ZnS, SiC, and $TiS_{1.7}$ polytypes. These methods are extremely sensitive to experimental errors in the intensities.

9.2.1.8. *Stacking faults in close-packed structures*

The two alternative positions for the stacking of successive close-packed layers give rise to the possibility of occurrence of faults where the stacking rule is broken without violating the law of close packing. Such faults are frequently observed in crystals of polytypic materials as well as close-packed martensites of cobalt, noble-metal-based and certain iron-based alloys (Andrade, Chandrasekaran & Delaey 1984; Kabra, Pandey & Lele, 1988*a*; Nishiyama, 1978; Pandey, 1988).

The classical method of classifying stacking faults in 2*H* and 3*C* structures as growth and deformation types, depending on whether the fault has resulted as an accident during growth or by shear through the vector **s**, leads to considerable ambiguities since the same fault configuration can result from more than one physical process. For a detailed account of the limitations of the notations based on the process of formation, the reader is referred to the articles by Pandey (1984*a*) and Pandey & Krishna (1982*b*).

Frank (1951) has classified stacking faults as intrinsic or extrinsic purely on geometrical considerations. In intrinsic faults, the perfect stacking sequence on each side of the fault extends right up to the contact plane of the two crystal halves while in extrinsic faults the contact plane does not belong to the stacking sequence on either side of it. In intrinsic faults, the contact plane may be an atomic or non-atomic plane whereas in extrinsic faults the contact plane is always an atomic plane. Instead of contact plane, one can use the concept of fault plane defined with respect to the initial stacking sequence. This system of classification is preferable to that based on the process of formation. However, the terms intrinsic and extrinsic have been used in the literature in a very restricted sense by associating these with the precipitation of vacancies and interstitials, respectively (see, for example, Weertman & Weertman, 1984). While the precipitation of vacancies may lead to intrinsic fault configuration, this is by no means the only process by which intrinsic faults can result. For example, there are geometrically 18 possible intrinsic fault configurations in the 6*H* (33) structure (Pandey & Krishna, 1975) but only two of these can result from the precipitation of vacancies. Similarly, layer-displacement faults involved in SiC transformations are extrinsic type but do not result from the precipitation of interstitials (see Pandey, Lele & Krishna, 1980*a*,*b*,*c*; Kabra, Pandey & Lele, 1986). It is therefore desirable not to associate the geometrical notation of Frank with any particular process of formation.

The intrinsic–extrinsic scheme of classification of faults when used in conjunction with the concept of assigning subscripts to different close-packed layers (Prasad & Lele, 1971; Pandey & Krishna, 1976*b*) can provide a very compact and unique way of representing intrinsic fault configurations even in long-period structures (Pandey, 1984*b*). We shall briefly explain this notation in relation to one hexagonal (6*H*) and one rhombohedral (9*R*) structure.

In the 6*H* (*ABCACB*, ... or *hkkhkk*) structure, six kinds of layers that can be assigned subscripts 0, 1, 2, 3, 4, and 5 need to be distinguished (Pandey, 1984*b*). Choosing the 0-type layer in '*h*' configuration such that the layer next to it is related through the shift vector $+\mathbf{s}$ (which causes cyclic $A \rightarrow B \rightarrow C \rightarrow A$ shift), the perfect 6*H* structure can be written as

$$\begin{array}{cccccccccccc} & h & k & k & h & k & k & h & k & k & h & k & k & \\ \ldots & A_0 & B_1 & C_2 & A_3 & C_4 & B_5 & A_0 & B_1 & C_2 & A_3 & C_4 & B_5 & \ldots. \\ & +\mathbf{s} & +\mathbf{s} & +\mathbf{s} & -\mathbf{s} & -\mathbf{s} & -\mathbf{s} & +\mathbf{s} & +\mathbf{s} & +\mathbf{s} & -\mathbf{s} & -\mathbf{s} & & \end{array}$$

There are six crystallographically equivalent ways of writing this structure with the first layer in position *A*: (i) $A_0B_1C_2A_3C_4B_5$; (ii) $A_1B_2C_3B_4A_5C_0$; (iii) $A_2B_3A_4C_5B_0C_1$; (iv) $A_3C_4B_5A_0B_1C_2$; (v) $A_4C_5B_0C_1A_2B_3$; and (vi) $A_5C_0A_1B_2C_3B_4$. Similarly, there are six ways of writing the 6*H* structure with the starting layer in position *B* or *C*. Since an intrinsic fault marks the beginning of a fresh 6*H* sequence, there can be 36 possible intrinsic fault configurations in the 6*H* (*ABCACB*, ...) structure. All these intrinsic fault configurations can be described by symbols like $I_{r,s}$, where *r* and *s* stand for the subscript of the layer on the left- and right-hand sides of the fault plane while *I* represents intrinsic. Knowing the two symbols (*r* and *s*), one can write down the complete *ABC* stacking sequence. It may be noted that, of the 36 possible intrinsic fault configurations, only 14 are crystallographically indistinguishable (for details, see Pandey, 1984*b*). This notation can be used for any hexagonal polytype and requires only the identification of various layer types in the structure. For rhombohedral polytypes, one must consider the layer types in both the obverse and the reverse settings. For example, six layer types need to be distinguished in the 9*R* (*hhk*) structure:

Obverse:

$$\begin{array}{cccccccccc} & h & h & k & h & h & k & h & h & k & \\ \ldots & A_0 & B_1 & A_2 & C_0 & A_1 & C_2 & B_0 & C_1 & B_2 & \ldots; \\ & +\mathbf{s} & -\mathbf{s} & -\mathbf{s} & +\mathbf{s} & -\mathbf{s} & -\mathbf{s} & +\mathbf{s} & -\mathbf{s} & & \end{array}$$

Table 9.2.1.3. *Intrinsic fault configurations in the 6H* $(A_0B_1C_2A_3C_4B_5, \ldots)$ *structure*

Fault configuration *ABC* sequence	Subscript notation
$\ldots A\,B\,C\,A\,C\,B\,A_0 \mid C_0\,A\,B\,C\,B\,A\,C \ldots$	$I_{0,0}$
$\ldots A\,B\,C\,A\,C\,B\,A_0 \mid C_1\,A\,B\,A\,C\,B\,C \ldots$	$I_{0,1}$
$\ldots A\,B\,C\,A\,C\,B\,A_0 \mid C_2\,A\,C\,B\,A\,B\,C \ldots$	$I_{0,2}$
$\ldots A\,B\,C\,A\,C\,B\,A_0 \mid C_3\,B\,A\,C\,A\,B\,C \ldots$	$I_{0,3}$
$\ldots A\,B\,C\,A\,C\,B\,A_0 \mid C_4\,B\,A\,B\,C\,A\,C \ldots$	$I_{0,4}$
$\ldots A\,B\,C\,A\,C\,B\,A_0 \mid C_5\,B\,C\,A\,B\,A\,C \ldots$	$I_{0,5}$
$\ldots A\,B\,C\,A\,C\,B\,A\,B_1 \mid A_0\,B\,C\,A\,C\,B\,A \ldots$	$I_{1,0}$
$\ldots A\,B\,C\,A\,C\,B\,A\,B_1 \mid A_1\,B\,C\,B\,A\,C\,A \ldots$	$I_{1,1}$
$\ldots A\,B\,C\,A\,C\,B\,A\,B_1 \mid A_2\,B\,A\,C\,B\,C\,A \ldots$	$I_{1,2}$
$\ldots A\,B\,C\,A\,C\,B\,A\,B_1 \mid A_3\,C\,B\,A\,B\,C\,A \ldots$	$I_{1,3}$
$\ldots A\,B\,C\,A\,C\,B\,A\,B_1 \mid A_4\,C\,B\,C\,A\,B\,A \ldots$	$I_{1,4}$
$\ldots A\,B\,C\,A\,C\,B\,A\,B_1 \mid A_5\,C\,A\,B\,C\,B\,A \ldots$	$I_{1,5}$
$\ldots A\,B\,C\,A\,C\,B\,A\,B\,C_2 \mid B_0\,C\,A\,B\,A\,C\,B \ldots$	$I_{2,0}$
$\ldots A\,B\,C\,A\,C\,B\,A\,B\,C_2 \mid B_1\,C\,A\,C\,B\,A\,B \ldots$	$I_{2,1}$
$\ldots A\,B\,C\,A\,C\,B\,A\,B\,C_2 \mid B_2\,C\,B\,A\,C\,A\,B \ldots$	$I_{2,2}$
$\ldots A\,B\,C\,A\,C\,B\,A\,B\,C_2 \mid B_3\,A\,C\,B\,C\,A\,B \ldots$	$I_{2,3}$
$\ldots A\,B\,C\,A\,C\,B\,A\,B\,C_2 \mid B_4\,A\,C\,A\,B\,C\,B \ldots$	$I_{2,4}$
$\ldots A\,B\,C\,A\,C\,B\,A\,B\,C_2 \mid B_5\,A\,B\,C\,A\,C\,B \ldots$	$I_{2,5}$

Notes:

(1) Dotted vertical lines represent the location of the fault plane with respect to the initial stacking sequence on the left-hand side.

(2) $I_{0,1}$ and $I_{2,3}$, $I_{0,2}$ and $I_{1,3}$, $I_{1,1}$ and $I_{2,2}$, and $I_{1,4}$ and $I_{2,5}$ are crystallographically equivalent.

Table 9.2.1.4. *Intrinsic fault configurations in the 9R ($A_0B_1A_2C_0A_1C_2B_0C_1B_2, \ldots$) structure*

Fault configuration *ABC* sequence	Subscript notation
$\ldots A\ B\ A\ C\ A\ C\ B\ C\ B\ A_0 \mid C_0\ A\ C\ B\ C\ B\ A\ B\ A \ldots$	$I_{0,0}$
$\ldots A\ B\ A\ C\ A\ C\ B\ C\ B\ A_0 \mid C_1\ B\ A\ B\ A\ C\ A\ C\ B \ldots$	$I_{0,1}$
$\ldots A\ B\ A\ C\ A\ C\ B\ C\ B\ A_0 \mid C_2\ B\ C\ B\ A\ B\ A\ C\ A \ldots$	$I_{0,2}$
$\ldots A\ B\ A\ C\ A\ C\ B\ C\ B\ A_0 \mid C_{\bar{0}}\ B\ C\ A\ C\ A\ B\ A\ B \ldots$	$I_{0,\bar{0}}$
$\ldots A\ B\ A\ C\ A\ C\ B\ C\ B\ A_0 \mid C_{\bar{1}}\ A\ B\ A\ B\ C\ B\ C\ A \ldots$	$I_{0,\bar{1}}$
$\ldots A\ B\ A\ C\ A\ C\ B\ C\ B\ A_0 \mid C_{\bar{2}}\ A\ C\ A\ B\ A\ B\ C\ B \ldots$	$I_{0,\bar{2}}$
$\ldots A\ B\ A\ C\ A\ C\ B\ C\ B\ A\ B_1 \mid C_0\ A\ C\ B\ C\ B\ A\ B\ A \ldots$	$I_{1,0}$
$\ldots A\ B\ A\ C\ A\ C\ B\ C\ B\ A\ B_1 \mid C_1\ B\ A\ B\ A\ C\ A\ C\ B \ldots$	$I_{1,1}$
$\ldots A\ B\ A\ C\ A\ C\ B\ C\ B\ A\ B_1 \mid C_2\ B\ C\ B\ A\ B\ A\ C\ A \ldots$	$I_{1,2}$
$\ldots A\ B\ A\ C\ A\ C\ B\ C\ B\ A\ B_1 \mid C_{\bar{0}}\ B\ C\ A\ C\ A\ B\ A\ B \ldots$	$I_{1,\bar{0}}$
$\ldots A\ B\ A\ C\ A\ C\ B\ C\ B\ A\ B_1 \mid C_{\bar{1}}\ A\ B\ A\ B\ C\ B\ C\ A \ldots$	$I_{1,\bar{1}}$
$\ldots A\ B\ A\ C\ A\ C\ B\ C\ B\ A\ B_1 \mid C_{\bar{2}}\ A\ C\ A\ B\ A\ B\ C\ B \ldots$	$I_{1,\bar{2}}$
$\ldots A\ B\ A\ C\ A\ C\ B\ C\ B\ A\ B\ A_2 \mid B_0\ C\ B\ A\ B\ A\ C\ A\ C \ldots$	$I_{2,0}$
$\ldots A\ B\ A\ C\ A\ C\ B\ C\ B\ A\ B\ A_2 \mid B_1\ A\ C\ A\ C\ B\ C\ B\ A \ldots$	$I_{2,1}$
$\ldots A\ B\ A\ C\ A\ C\ B\ C\ B\ A\ B\ A_2 \mid B_2\ A\ B\ A\ C\ A\ C\ B\ C \ldots$	$I_{2,2}$
$\ldots A\ B\ A\ C\ A\ C\ B\ C\ B\ A\ B\ A_2 \mid B_{\bar{0}}\ A\ B\ C\ B\ C\ A\ C\ A \ldots$	$I_{2,\bar{0}}$
$\ldots A\ B\ A\ C\ A\ C\ B\ C\ B\ A\ B\ A_2 \mid B_{\bar{1}}\ C\ A\ C\ A\ B\ A\ B\ C \ldots$	$I_{2,\bar{1}}$
$\ldots A\ B\ A\ C\ A\ C\ B\ C\ B\ A\ B\ A_2 \mid B_{\bar{2}}\ C\ B\ C\ A\ C\ A\ B\ A \ldots$	$I_{2,\bar{2}}$

Note: $I_{0,\bar{0}}$ and $I_{1,\bar{1}}$, $I_{0,\bar{1}}$ and $I_{1,\bar{2}}$, $I_{0,\bar{2}}$ and $I_{2,\bar{1}}$, and $I_{1,2}$ and $I_{2,0}$ are crystallographically equivalent.

Reverse:

$$\begin{array}{cccccccccc} & h & h & k & h & h & k & h & h & k & \\ \ldots & A_{\bar{0}} & C_{\bar{1}} & A_{\bar{2}} & B_{\bar{0}} & A_{\bar{1}} & B_{\bar{2}} & C_{\bar{0}} & B_{\bar{1}} & C_{\bar{2}} & \ldots . \\ & -\mathbf{s} & +\mathbf{s} & +\mathbf{s} & -\mathbf{s} & +\mathbf{s} & +\mathbf{s} & -\mathbf{s} & +\mathbf{s} & & \end{array}$$

In the obverse setting, we choose the origin layer (0 type) in the *h* configuration such that the next layer is cyclically shifted whereas in the reverse setting the origin layer ($\bar{0}$ type) in the *h* configuration is related to the next layer through an anticyclic shift. Tables 9.2.1.3 and 9.2.1.4 list the crystallographically unique intrinsic fault configurations in the 6*H* and 9*R* structures.

9.2.1.8.1. *Structure determination of one-dimensionally disordered crystals*

Statistical distribution of stacking faults in close-packed structures introduces disorder along the stacking axis of the close-packed layers. As a result, one observes on a single-crystal diffraction pattern not only normal Bragg scattering near the nodes of the reciprocal lattice of the average structure but also continuous diffuse scattering between the nodes owing to the incomplete destructive interference of scattered rays. Just like the extra polytype reflections, the diffuse streaks are also confined to only those rows for which $h - k \neq 0 \bmod 3$. A complete description of the real structure of such one-dimensionally disordered polytypes requires knowledge of the average structure as well as a statistical specification of the fluctuations due to stacking faults in the electron-density distribution of the average structure. This cannot be accomplished by the usual consideration of the normal Bragg reflections alone but requires a careful analysis of the diffuse intensity distribution as well (Pandey, Kabra & Lele, 1986).

The first step in the structure determination of one-dimensionally disordered structures is the specification of the geometry of stacking faults and their distribution, both of which require postulation of the physical processes responsible for their formation. An entirely random distribution of faults may result during the layer-by-layer growth of a crystal (Wilson, 1942) or during plastic deformation (Paterson, 1952). On the other hand, when faults bring about the change in the stacking sequence of layers during solid-state transformations, their distribution is non-random (Pandey, Lele & Krishna, 1980*a*,*b*,*c*; Pandey & Lele, 1986*a*,*b*; Kabra, Pandey & Lele, 1986). Unlike growth faults, which are accidentally introduced in a sequential fashion from one end of the stack of layers to the other during the actual crystal growth, stacking faults involved in solid-state transformations are introduced in a random space and time sequence (Kabra, Pandey & Lele, 1988*b*). Since the pioneering work of Wilson (1942), several different techniques have been advanced for the calculation of intensity distributions along diffuse streaks making use of Markovian chains, random walk, stochastic matrices, and the Paterson function for random and non-random distributions of stacking faults on the assumption that these are introduced in a sequential fashion (Hendricks & Teller, 1942; Jagodzinski 1949*a*,*b*; Kakinoki & Komura, 1954; Johnson, 1963; Prasad & Lele, 1971; Cowley, 1976; Pandey, Lele & Krishna, 1980*a*,*b*). The limitations of these methods for situations where non-randomly distributed faults are introduced in the random space and time sequence have led to the use of Monte Carlo techniques for the numerical calculation of pair correlations whose Fourier transforms directly yield the intensity distributions (Kabra & Pandey, 1988).

The correctness of the proposed model for disorder can be verified by comparing the theoretically calculated intensity distributions with those experimentally observed. This step is in principle analogous to the comparison of the observed Bragg intensities with those calculated for a proposed structure in the structure determination of regularly ordered layer stackings. This comparison cannot, however, be performed in a straightforward manner for one-dimensionally disordered crystals due to special problems in the measurement of diffuse intensities using a single-crystal diffractometer, stemming from incident-beam divergence, finite size of the detector slit, and multiple scattering. The problems due to incident-beam divergence in the measurement of the diffuse intensity distributions were first

pointed out by Pandey & Krishna (1977) and suitable correction factors have recently been derived by Pandey, Prasad, Lele & Gauthier (1987). A satisfactory solution to the problem of structure determination of one-dimensionally disordered stackings must await proper understanding of all other factors that may influence the true diffraction profiles.

9.2.2. Layer stacking in general polytypic structures (By S. Ďurovič)

9.2.2.1. *The notion of polytypism*

The common property of the structures described in Section 9.2.1 was the stacking ambiguity of adjacent layer-like structural units. This has been explained by the geometrical properties of close packing of equal spheres, and the different modifications thus obtained have been called *polytypes*.

This phenomenon was first recognized by Baumhauer (1912, 1915) as a result of his investigations of many SiC single crystals by optical goniometry. Among these, he discovered three *types* and his observations were formulated in five statements:

(1) all three types originate simultaneously in the same melt and seemingly also under the same, or nearly the same, conditions;

(2) they can be related in a simple way to the same axial ratio (each within an individual primary series);

(3) any two types (I and II, II and III) have certain faces in common but, except the basal face, there is no face occurring simultaneously in all three types;

(4) the crystals belonging to different, but also to all three, types often form intergrowths with parallel axes;

(5) any of the three types exhibits a typical X-ray diffraction pattern and thus also an individual molecular or atomic structure.

Baumhauer recognized the special role of these *types* within modifications of the same substance and called this phenomenon *polytypism* – a special case of polymorphism. The later determination of the crystal structures of Baumhauer's three types indicated that his results can be interpreted by a family of structures consisting of identical layers with hexagonal symmetry and differing only in their stacking mode.

The stipulation that the individual polytypes grow from the same system and under (nearly) the same conditions influenced for years the investigation of polytypes because it logically led to the question of their growth mechanism.

In the following years, many new polytypic substances have been found. Their crystal structures revealed that polytypism is restricted neither to close packings nor to heterodesmic 'layered structures' (*e.g.* CdI_2 or GaSe; *cf.* homodesmic SiC or ZnS; see §§9.2.1.2.2 to 9.2.1.2.4), and that the reasons for a stacking ambiguity lie in the crystal chemistry – in all cases the geometric nearest-neighbour relations between adjacent layers are preserved. The preservation of the bulk chemical composition was not questioned.

Some discomfort has arisen from refinements of the structures of various phyllosilicates. Here especially the micas exhibit a large variety of isomorphous replacements and it turns out that a certain chemical composition stabilizes certain polytypes, excludes others, and that the layers constituting polytypic structures need not be of the same kind. But subsequently the opinion prevailed that the sequence of individual kinds of layers in polytypes of the same family should remain the same and that the relative positions of adjacent layers cannot be completely random (*e.g.* Zvyagin, 1988). The postulates declared mixed-layer and turbostratic structures as non-polytypic. All this led to certain controversies about the notion of polytypism. While Thompson (1981) regards polytypes as 'arising through different ways of stacking structurally compatible tabular units ... [provided that this] ... should not alter the chemistry of the crystal as a whole', Angel (1986) demands that 'polytypism arises from different modes of stacking of one or more structurally compatible modules', dropping thus any chemical constraints and allowing also for rod- and block-like modules.

The present official definition (Guinier *et al.*, 1984) reads:

> ''An element or compound is *polytypic* if it occurs in several different structural modifications, each of which may be regarded as built up by stacking layers of (nearly) identical structure and composition, and if the modifications differ only in their stacking sequence. Polytypism is a special case of polymorphism: the two-dimensional translations within the layers are (essentially) preserved whereas the lattice spacings normal to the layers vary between polytypes and are indicative of the stacking period. No such restrictions apply to polymorphism.
>
> *Comment*: The above definition is designed to be sufficiently general to make polytypism a useful concept. There is increasing evidence that some polytypic structures are characterized either by small deviations from stoichiometry or by small amounts of impurities. (In the case of certain minerals like clays, micas and ferrites, deviations in composition up to 0.25 atoms per formula unit are permitted within the same polytypic series: two layer structures that differ by more than this amount should not be called polytypic.) Likewise, layers in different polytypic structures may exhibit slight structural differences and may not be isomorphic in the strict crystallographic sense.
>
> The *Ad-Hoc* Committee is aware that the definition of polytypism above is probably too wide since it includes, for example, the turbostratic form of graphite as well as mixed-layer phyllosilicates. However, the sequence and stacking of layers in a polytype are always subject to well-defined limitations. On the other hand, a more general definition of polytypism that includes 'rod' and 'block' polytypes may become necessary in the future.''

This definition was elaborated as a compromise between members of the IUCr *Ad-Hoc* Committee on the Nomenclature of Disordered, Modulated and Polytype Structures. It is a slightly modified definition proposed by the IMA/IUCr Joint Committee on Nomenclature (Bailey *et al.*, 1977), which was the target of Angel's (1986) objections.

The official definition has indeed its shortcomings, but not so much in its restrictiveness concerning the chemical composition and structural rigidity of layers, because this can be overcome by a proper degree of abstraction (see below). More critical is the fact that it is not 'geometric' enough. It specifies neither the 'layers' (except for their two-dimensional periodicity), nor the limitations concerning their sequence and stacking mode, and it does not state the conditions under which a polytype belongs to a family.

Very impressive evidence that even polytypes that are in keeping with the first Baumhauer's statement may not have exactly the same composition and the structure of their constituting layers *cannot* be identical has been provided by studies on SiC carried out at the Leningrad Electrotechnical Institute (Sorokin, Tairov, Tsvetkov & Chernov, 1982; Tsvetkov, 1982). They indicate also that each periodic polytype is *sensu stricto* an individual polymorph. Therefore, it appears that the question whether some *real* polytypes belong to the same

family depends mainly on the idealization and/or abstraction level, *relevant to a concrete purpose*.

This very idealization and/or abstraction process caused the term *polytype* to become also an *abstract notion* meaning a *structural type* with relevant geometrical properties,* belonging to an abstract family whose members consist of layers with identical structure and keep identical bulk composition. Such an abstract notion lies at the root of all systemization and classification schemes of polytypes.

A still higher degree of abstraction has been achieved by Dornberger-Schiff (1964, 1966, 1979) who abstracted from chemical composition completely and investigated the manifestation of crystallochemical reasons for polytypism in the *symmetry of layers* and *symmetry relations between layers*. Her theory of OD (order–disorder) structures is thus a theory of symmetry of polytypes, playing here a role similar to that of group theory in traditional crystallography. In the next section, a brief account of basic terms, definitions, and logical constructions of OD theory will be given, together with its contribution to a geometrical definition of polytypism.

9.2.2.2. *Symmetry aspects of polytypism*

9.2.2.2.1. *Close packing of spheres*

Polytypism of structures based on close packing of equal spheres (note this idealization) is explained by the fact that the spheres of any layer can be placed *either* in all the voids ∇ of the preceding layer, *or* in all the voids $\triangle$ – not in both because of steric hindrance (Section 9.2.1, Fig. 9.2.1.1).

A closer look reveals that the two voids are *geometrically* (but not translationally) *equivalent*. This implies that the two possible pairs of adjacent layers, say *AB* and *AC*, are geometrically equivalent too – this equivalence is brought about *e.g.* by a reflection in any plane perpendicular to the layers and passing through the centres of mutually contacting spheres *A*: such a reflection transforms the layer *A* into itself, and *B* into *C*, and *vice versa*. Another important point is that the symmetry proper of any layer is described by the layer group $P(6/m)mm$,† and that the relative position of any two adjacent layers is such that only some of the 24 symmetry operations of that layer group remain valid for the pair. It is easy to see that 12 out of the total of 24 transformations do not change the z coordinate of any starting point, and that these operations constitute a subgroup of the index [2]. These are the so-called τ *operations*. The remaining 12 operations change any z into $-z$, thus turning the layer upside down; they constitute a coset. The latter are called ρ *operations*. Out of the 12 τ operations, only 6 are valid for the layer pair. One says that only these 6 operations have a *continuation* in the adjacent layer. Let us denote the general multiplicity of the group of τ operations of a single layer by N, and that of the subgroup of these operations with a continuation in the adjacent layer by F: then the number Z of positions of the adjacent layer leading to geometrically equivalent layer pairs is given by $Z = N/F$ (Dornberger-Schiff, 1964, pp. 32 ff.); in our case, $Z = 12/6 = 2$ (Fig. 9.2.2.1). This is the so-called *NFZ relation*, valid with only minor alterations for all categories of OD structures (§9.2.2.2.7). It follows that all conceivable structures based on close packing of equal spheres are built on the same symmetry principle: they consist of equivalent layers (*i.e.* layers of the same kind) and of equivalent layer pairs, and, in keeping with these stipulations, any layer can be stacked onto its predecessor in two ways. Keeping in mind that the layer pairs that are geometrically equivalent are also energetically equivalent, and neglecting in the first approximation the interactions between a given layer and the next-but-one layer, we infer that all structures built according to these principles are also energetically equivalent and thus equally likely to appear.

It is important to realize that the above symmetry considerations hold not only for close packing of spheres but also for *any conceivable structure* consisting of two-dimensionally periodic layers with symmetry $P(6/m)mm$ and containing pairs of adjacent layers with symmetry $P(3)m1$. Moreover, the OD theory sets a quantitative stipulation for the relation between any two adjacent layers: they have to remain *geometrically equivalent* in any polytype belonging to a family. This is far more exact than the description: 'the stacking of layers is such that it preserves the nearest-neighbour relationships'.

9.2.2.2.2. *Polytype families and OD groupoid families*

All polytypes of a substance built on the same *structural principle* are said to belong to the same *family*. All polytypic structures, even of different substances, built according to the same *symmetry principle* also belong to a family, but different from the previous one since it includes structures of various polytype families, *e.g.* SiC, ZnS, AgI, which differ in their composition, lattice dimensions, *etc*. Such a family has been called an *OD groupoid family*; its members differ only in the relative distribution of *coincidence operations** describing the respective symmetries, irrespective of the crystallochemical content. These coincidence operations can be *total* or *partial* (local) and their set constitutes a groupoid (Dornberger-Schiff, 1964, pp. 16 ff.; Fichtner, 1965, 1977). Any polytype (abstract) belonging to such a family has its own stacking of layers, and its symmetry can be described by the appropriate individual groupoid. Strictly speaking, these groupoids are the members of an OD groupoid family. Let us recall that any space group

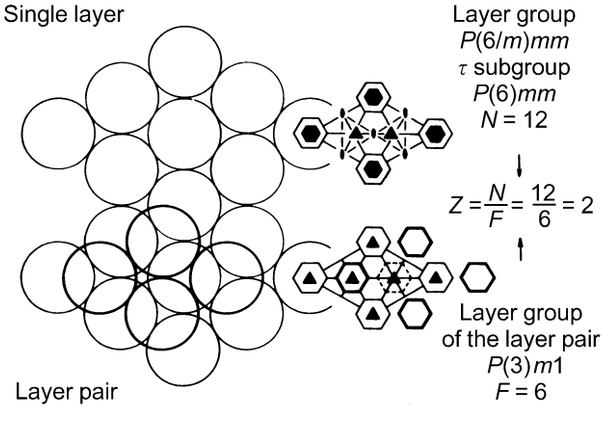

Fig. 9.2.2.1. Symmetry interpretation of close packings of equal spheres. The layer group of a single layer, the subgroup of its τ operations, and the number of asymmetric units N per unit mesh of the former, are given at the top right. The τ operations that have a continuation for the pair of adjacent layers, the layer group of the pair, and the value of F are indicated at the bottom right.

* This is an interesting example of how a development in a scientific discipline influences semantics: *e.g.* when speaking of a 6*H* polytype of SiC, one has very often in mind a characteristic sequence of Si–C layers rather than deviations from stoichiometry, presence and distribution of foreign atoms, distortion of coordination tetrahedra, *etc*.

† The direction in which there is no periodicity is indicated by parentheses (Dornberger-Schiff, 1959).

* A coincidence operation is a space transformation (called also *isometric mapping*, *isometry*, or *motion*), which preserves distances between any two points of the given object.

consists of total coincidence operations only, which therefore become the symmetry operations for the entire structure.

9.2.2.2.3. *MDO polytypes*

Any family of polytypes theoretically contains an infinite number of periodic (Ross, Takeda & Wones, 1966; Mogami, Nomura, Miyamoto, Takeda & Sadanaga, 1978; McLarnan, 1981*a*,*b*,*c*) and non-periodic structures. The periodic polytypes, in turn, can again be subdivided into two groups, the 'privileged' polytypes and the remaining ones, and it depends on the approach as to how this is done. Experimentalists single out those polytypes that occur most frequently, and call them *basic*. Theorists try to predict basic polytypes, *e.g.* by means of geometrical and/or crystallochemical considerations. Such polytypes have been called *simple, standard*, or *regular*. Sometimes the agreement is very good, sometimes not. The OD theory pays special attention to those polytypes in which *all layer triples, quadruples, etc.*, are geometrically equivalent or, at least, which contain the smallest possible number of *kinds* of these units. They have been called polytypes with *maximum degree of order*, or *MDO polytypes*. The general philosophy behind the MDO polytypes is simple: all interatomic bonding forces decrease rapidly with increasing distance. Therefore, the forces between atoms of adjacent layers are decisive for the build-up of a polytype. Since the pairs of adjacent layers remain geometrically equivalent in all polytypes of a given family, these polytypes are in the first approximation also energetically equivalent. However, if the longer-range interactions are also considered, then it becomes evident that layer triples such as *ABA* and *ABC* in close-packed structures are, in general, energetically non-equivalent because they are also geometrically non-equivalent. Even though these forces are much weaker than those between adjacent layers, they may not be negligible and, therefore, under given crystallization conditions either one or the other kind of triples becomes energetically more favourable. It will occur again and again in the polytype thus formed, and not intermixed with the other kind. Such structures are – as a rule – sensitive to conditions of crystallization, and small fluctuations of these may reverse the energetical preferences, creating stacking faults and twinnings. This is why many polytypic substances exhibit non-periodicity.

As regards the close packing of spheres, the well known cubic and hexagonal polytypes *ABCABC*... and *ABAB*..., respectively, are MDO polytypes; the first contains only the triples *ABC*, the second only the triples *ABA*. Evidently, the MDO philosophy holds for a layer-by-layer rather than for a spiral growth mechanism. Since the symmetry principle of polytypic structures may differ considerably from that of close packing of equal spheres, the OD theory contains exact algorithms for the derivation of MDO polytypes in any category (Dornberger-Schiff, 1982; Dornberger-Schiff & Grell, 1982*a*).

9.2.2.2.4. *Some geometrical properties of OD structures*

As already pointed out, all relevant geometrical properties of a polytype family can be deduced from its symmetry principle. Let us thus consider a hypothetical simple family in which we shall disregard any concrete atomic arrangements and use geometrical figures with the appropriate symmetry instead.

Three periodic polytypes are shown in Fig. 9.2.2.2 (left-hand side). Any member of this family consists of equivalent layers perpendicular to the plane of the drawing, with symmetry $P(1)m1$. The symmetry of layers is indicated by isosceles triangles with a mirror plane [*.m.*]. All pairs of adjacent layers are also equivalent, no matter whether a layer is shifted by $+b/4$ or $-b/4$ relative to its predecessor, since the reflection across [*.m.*] transforms any given layer into itself and the adjacent layer from one possible position into the other. These two positions follow also from the *NFZ* relation: $N = 2$, $F = 1$ [the layer group of the pair of adjacent layers is $P(1)11$] and thus $Z = 2$.

The layers are all equivalent and accordingly there must also be two coincidence operations transforming any layer into the adjacent one. The first operation is evidently the translation, the second is the glide reflection. If any of these becomes total for the remaining part of the structure, we obtain a polytype with all layer triples equivalent, *i.e.* a MDO polytype. The polytype (*a*) (Fig. 9.2.2.2) is one of them: the translation $\mathbf{t} = \mathbf{a}_0 + \mathbf{b}/4$ is the total operation ($|\mathbf{a}_0|$ is the distance between adjacent layers). It has basis vectors $\mathbf{a}_1 = \mathbf{a}_0 + \mathbf{b}/4$, $\mathbf{b}_1 = \mathbf{b}$, $\mathbf{c}_1 = \mathbf{c}$, space group $P111$, Ramsdell symbol $1A$,* Hägg symbol $|+|$. This polytype also has its enantiomorphous counterpart with Hägg symbol $|-|$. In the other polytype (*b*) (Fig. 9.2.2.2), the glide reflection is the total operation. The basis vectors of the polytype are

* According to Guinier *et al.* (1984), triclinic polytypes should be designated *A* (anorthic) in their Ramsdell symbols.

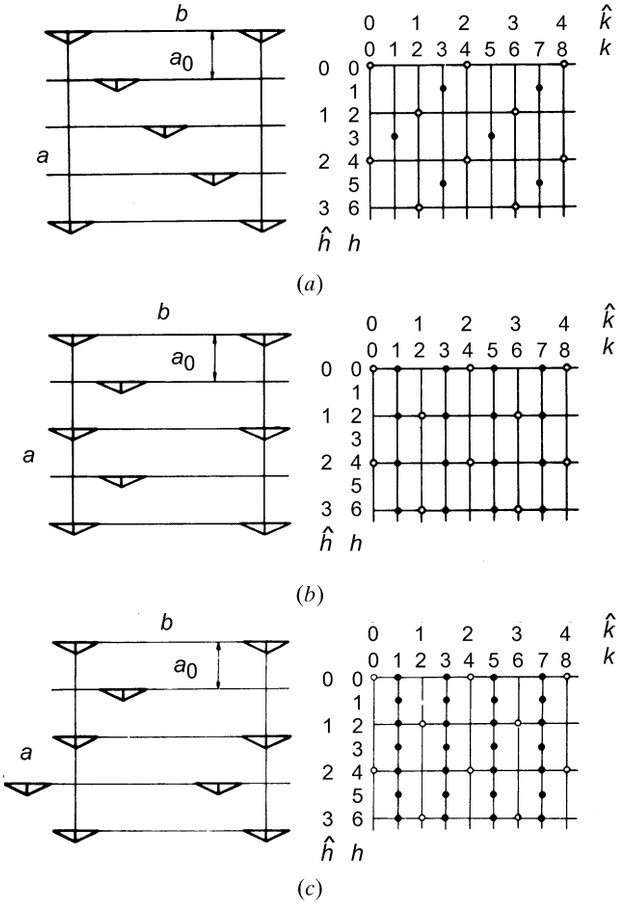

Fig. 9.2.2.2. Schematic representation of three structures belonging to the OD groupoid family $P(1)m1|1$, $y = 0.25$ (left). The layers are perpendicular to the plane of the drawing and their constituent atomic configurations are represented by isosceles triangles with symmetry [*.m.*]. All structures are related to a common orthogonal four-layer cell with $\mathbf{a} = 4\mathbf{a}_0$. The $hk0$ nets in reciprocal space corresponding to these structures are shown on the right and the diffraction indices refer also to the common cell. Family diffractions common to all members of this family ($k = 2\hat{k}$) and the characteristic diffractions for individual polytypes ($k = 2k + 1$) are indicated by open and solid circles, respectively.

$\mathbf{a}_2 = 2\mathbf{a}_0$, $\mathbf{b}_2 = \mathbf{b}$, $\mathbf{c}_2 = \mathbf{c}$, space group $P1a1$, Ramsdell symbol $2M$, Hägg symbol $|+-|$. The equivalence of all layer triples in either of these polytypes is evident. The third polytype (*c*) (Fig. 9.2.2.2) is not a MDO polytype because it contains two kinds of layer triples, whereas it is possible to construct a polytype of this family containing only a selection of these. The polytype is again monoclinic with basis vectors $\mathbf{a}_3 = 4\mathbf{a}_0$, $\mathbf{b}_3 = \mathbf{b}$, $\mathbf{c}_3 = \mathbf{c}$, space group $P1a1$, Ramsdell symbol $4M$, and Hägg symbol $|+--+|$.

Evidently, the partial mirror plane is crucial for the polytypism of this family. And yet the space group of none of its periodic members can contain it – simply because it can never become total. The space-group symbols thus leave some of the most important properties of periodic polytypes unnoticed. Moreover, the atomic coordinates of different polytypes expressed in terms of the respective lattice geometries cannot be immediately compared. And, finally, for non-periodic members of a family, a space-group symbol cannot be written at all. This is why the OD theory gives a *special symbol* indicating the symmetry proper of individual layers (λ symmetry) as well as the coincidence operations transforming a layer into the adjacent one (σ symmetry). The symbol of the OD groupoid family of our hypothetical example thus consists of two lines (Dornberger-Schiff, 1964, pp. 41 ff.; Fichtner, 1979*a*,*b*):

$$\begin{array}{llll} P(1) & m & 1 & \lambda \text{ symmetry} \\ \{(1) & a_2 & 1\} & \sigma \text{ symmetry,} \end{array}$$

where the unusual subscript 2 indicates that the glide reflection transforms the given layer into the subsequent one.

It is possible to write such a symbol for any OD groupoid family for equivalent layers, and thus also for the close packing of spheres. However, keeping in mind that the number of asymmetric units here is 24 (λ symmetry), one has to indicate also 24 σ operations, which is instructive but unwieldy. This is why Fichtner (1980) proposed simplified one-line symbols, containing full λ symmetry and only the rotational part of *any one* of the σ operations plus its translational components. Accordingly, the symbol of our hypothetical family reads: $P(1)m1|1,\ y = 0.25$; for the family of close packings of equal spheres: $P(6/m)mm|1,\ x = 2/3,\ y = 1/3$ (the layers are in both cases translationally equivalent and the rotational part of a translation is the identity).

An OD groupoid family symbol should not be confused with a *polytype symbol*, which gives information about the structure of an individual polytype (Dornberger-Schiff, Ďurovič & Zvyagin, 1982; Guinier *et al.*, 1984).

9.2.2.2.5. *Diffraction pattern – structure analysis*

Let us now consider schematic diffraction patterns of the three structures on the right-hand side of Fig. 9.2.2.2. It can be seen that, while being in general different, they contain a common subset of diffractions with $k = 2\hat{k}$ – these, normalized to a constant number of layers, have the same distribution of intensities and monoclinic symmetry. This follows from the fact that they correspond to the so-called *superposition structure* with basis vectors $\mathbf{A} = 2\mathbf{a}_0$, $\mathbf{B} = \mathbf{b}/2$, $\mathbf{C} = \mathbf{c}$, and space group $C1m1$. It is a fictitious structure that can be obtained from any of the structures in Fig. 9.2.2.2 as a normalized sum of the structure in its given position and in a position shifted by $b/2$, thus

$$\hat{\rho}(xyz) = \tfrac{1}{2}[\rho(xyz) + \rho(x, y + 1/2, z)].$$

Evidently, this holds for all members of the family, including the non-periodic ones. In general, the superposition structure is obtained by simultaneous realization of all Z possible positions of all OD layers in any member of the family (Dornberger-Schiff, 1964, p. 54). As a consequence, its symmetry can be obtained by completing any of the family groupoids to a group (Fichtner, 1977). This structure is by definition periodic and *common to all members* of the family. Thus, the corresponding diffractions are also always sharp, common, and characteristic for the family. They are called *family diffractions*.

Diffractions with $k = 2\hat{k} + 1$ are characteristic for individual members of the family. They are sharp for periodic polytypes but appear as diffuse streaks for non-periodic ones. Owing to the C centring of the superposition structure, only diffractions with $\hat{h} + \hat{k} = 2n$ are present. It follows that $0\hat{k}\hat{l}$ diffractions are present only for $\hat{k} = 2n$, which, in an indexing referring to the actual **b** vector reads: $0kl$ present only for $k = 4n$. This is an example of non-space-group absences exhibited by many polytypic structures. They can be used for the determination of the OD groupoid family (Dornberger-Schiff & Fichtner, 1972).

There is no routine method for the determination of the structural principle of an OD structure. It is easiest when one has at one's disposal many different (at least two) periodic polytypes of the same family with structures solved by current methods. It is then possible to compare these structures, determine equivalent regions in them (Grell, 1984), and analyse partial symmetries. This results in an OD interpretation of the substance and a description of its polytypism.

Sometimes it is possible to arrive at an OD interpretation from one periodic structure, but this necessitates experience in the recognition of the partial symmetry and prediction of potential polytypism (Merlino, Orlandi, Perchiazzi, Basso & Palenzona, 1989).

The determination of the structural principle is complex if only disordered polytypes occur. Then – as a rule – the superposition structure is solved first by current methods. The actual structure of layers and relations between them can then be determined from the intensity distribution along diffuse streaks (for more details and references see Jagodzinski, 1964; Sedlacek, Kuban & Backhaus, 1987; Müller & Conradi, 1986). High-resolution electron microscopy can also be successfully applied – see Subsection 9.2.2.4.

9.2.2.2.6. *The vicinity condition*

A polytype family contains periodic as well as non-periodic members. The latter are as important as the former, since the very fact that they can be non-periodic carries important crystallochemical information. Non-periodic polytypes do not comply with the classical definition of crystals, but we believe that this definition should be generalized to include rather than exclude non-periodic polytypes from the world of crystals (Dornberger-Schiff & Grell, 1982*b*). The OD theory places them, together with the periodic ones, in the hierarchy of the so-called *VC structures*. The reason for this is that all periodic structures, even the non-polytypic ones, can be thought of as consisting of *disjunct*, two-dimensionally periodic slabs, the *VC layers*, which are stacked together according to three rules called the *vicinity condition* (VC) (Dornberger-Schiff, 1964, pp. 29 ff., 1979; Dornberger-Schiff & Fichtner, 1972):

(α) VC layers are either geometrically equivalent or, if not, they are relatively few in kind;

(β) translation groups of all VC layers are either identical or they have a common subgroup;

(γ) equivalent sides of equivalent layers are faced by equivalent sides of adjacent layers so that the resulting pairs are equivalent [for a more detailed specification and explanation see Dornberger-Schiff (1979)].

If the stacking of VC layers is unambiguous, traditional three-dimensionally periodic structures result (*fully ordered structures*). *OD structures* are VC structures in which the stacking of VC layers is ambiguous at every layer boundary ($Z > 1$). The corresponding VC layers then become *OD layers*. OD layers are, in general, not identical with crystallochemical layers; they may contain half-atoms at their boundaries. In this context, they are analogous with unit cells in traditional crystallography, which may also contain parts of atoms at their boundaries. However, *the choice of OD layers is not absolute*: it depends on the polytypism, either actually observed or reasonably anticipated, on the degree of symmetry idealization, and other circumstances (Grell, 1984).

9.2.2.2.7. *Categories of OD structures*

Any OD layer is two-dimensionally periodic. Thus, a unit mesh can be chosen according to the conventional rules for the corresponding layer group; the corresponding vectors or their linear combinations (Zvyagin & Fichtner, 1986) yield the basis vectors parallel to the layer plane and thus also their lengths as units for fractional atomic coordinates. But, in general, there is no periodicity in the direction perpendicular to the layer plane and it is thus necessary to define the corresponding unit length in some other way. This depends on the symmetry principle of the family in question – or, more narrowly, on the *category* to which this family belongs.

OD structures can be built of *equivalent layers* or contain *layers of several kinds*. The rule (γ) of the VC implies that a projection of any OD structure – periodic or not – on the stacking direction is periodic. This period, called *repeat unit*, is the required unit length.

9.2.2.2.7.1. *OD structures of equivalent layers*

If the OD layers are equivalent then they are either all polar or all non-polar in the stacking direction. Any two adjacent polar layers can be related either by τ operations only, or by ρ operations only. For non-polar layers, the σ operations are both τ and ρ. Accordingly, there are *three categories* of OD structures of equivalent layers. They are shown schematically in Fig. 9.2.2.3; the character of the corresponding λ and σ operations is as follows (Dornberger-Schiff, 1964, pp. 24 ff.):

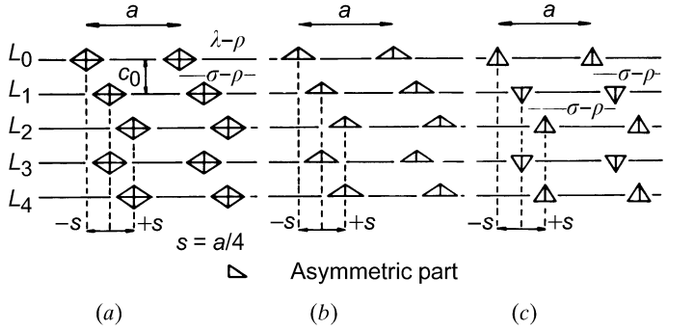

Fig. 9.2.2.3. Schematic examples of the three categories of OD structures consisting of equivalent layers (perpendicular to the plane of the drawing): (*a*) category I – OD layers non-polar in the stacking direction; (*b*) category II – polar OD layers, all with the same sense of polarity; (*c*) category III – polar OD layers with regularly alternating sense of polarity. The position of ρ planes is indicated.

	category I	category II	category III
λ operations	τ and ρ	τ	τ
σ operations	τ and ρ	τ	ρ

Category II is the simplest: the OD layers are polar and all with the same sense of polarity (they are τ-equivalent); our hypothetical example given in §9.2.2.2.4 belongs to this category. The layers can thus exhibit only one of the 17 polar layer groups. The projection of any vector between two τ-equivalent points in two adjacent layers on the stacking direction (perpendicular to the layer planes) is the repeat unit and it is denoted by $\mathbf{c}_0$, $\mathbf{a}_0$, or $\mathbf{b}_0$ depending on whether the basis vectors in the layer plane are **ab**, **bc**, or **ca**, respectively. The choice of origin in the stacking direction is arbitrary but preferably so that the z coordinates of atoms within a layer are positive. Examples are SiC, ZnS, and AgI.

OD layers in category I are non-polar and they can thus exhibit any of the 63 non-polar layer groups. Inspection of Fig. 9.2.2.3(*a*) reveals that the symmetry elements representing the λ–ρ operations (*i.e.* the operations turning a layer upside down) can lie only in one plane called the *layer plane*. Similarly, the symmetry elements representing the σ–ρ operations (*i.e.* the operations converting a layer into the adjacent one) also lie in one plane, located exactly halfway between two nearest layer planes. These two kinds of planes are called ρ planes. The distance between two nearest layer planes is the repeat unit c_0. Examples are close packing of equal spheres, GaSe, α-wollastonite (Yamanaka & Mori, 1981), β-wollastonite (Ito, Sadanaga, Takéuchi & Tokonami, 1969), $K_3[M(CN)_6]$ (Jagner, 1985), and many others.

The OD structures belonging to the above two categories contain pairs of adjacent layers, all equivalent. This does not apply for structures of category III, which consist of polar layers that are converted into their neighbours by ρ operations. It is evident (Fig. 9.2.2.3*c*) that two kinds of pairs of adjacent layers are needed to build any such structure. It follows that only even-numbered layers can be mutually τ-equivalent and the same holds for odd-numbered layers. There are only σ–ρ planes in these structures, and again they

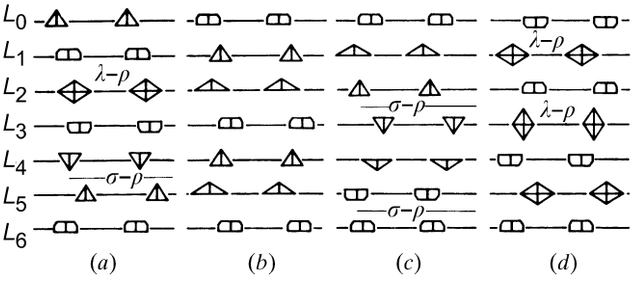

Fig. 9.2.2.4. Schematic examples of the four categories of OD structures consisting of more than one kind of layer (perpendicular to the plane of the drawing). Equivalent OD layers are represented by equivalent symbolic figures. (*a*) Category I – three kinds of OD layers: one kind (L_{2+5n}) is non-polar, the remaining two are polar. One and only one kind of non-polar layer is possible in this category. (*b*) Category II – three kinds of polar OD layers; their triples are polar and retain their sense of polarity in the stacking direction. (*c*) Category III – three kinds of polar OD layers; their triples are polar and regularly change their sense of polarity in the stacking direction. (*d*) Category IV – three kinds of OD layers: two kinds are non-polar (L_{1+4n} and L_{3+4n}), one kind is polar. Two and only two kinds of non-polar layers are possible in this category. The position of ρ planes is indicated.

are of two kinds; the origin can be placed in either of them. c_0 is the distance between two nearest ρ planes of the same kind, and slabs of this thickness contain two OD layers. There are three examples for this category known to date: foshagite (Gard & Taylor, 1960), γ-$Hg_3S_2Cl_2$ (Ďurovič, 1968), and 2,2-aziridinedicarboxamide (Fichtner & Grell, 1984).

9.2.2.2.7.2. *OD structures with more than one kind of layer*

If an OD structure consists of $N > 1$ kinds of OD layers, then it can be shown (Dornberger-Schiff, 1964, pp. 64 ff.) that it can fall into one of *four categories*, according to the polarity or non-polarity of its constituent layers and their sequence. These are shown schematically in Fig. 9.2.2.4; the character of the corresponding λ and σ operations is

	category I	category II	category III	category IV
λ operations	τ and ρ (one set) τ ($N-1$ sets)	τ (N sets)	τ (N sets)	τ and ρ (two sets) τ ($N-2$ sets)
σ operations	ρ (one set)	none	ρ (two sets)	none.

Here also category II is the simplest. The structures consist of N kinds of cyclically recurring polar layers whose sense of polarity remains unchanged (Fig. 9.2.2.4*b*). The choice of origin in the stacking direction is arbitrary; c_0 is the projection on this direction of the shortest vector between two τ-equivalent points – a slab of this thickness contains all N OD layers of different kinds. Examples are the structures of the serpentine–kaolin group.

Structures of category III also consist of polar layers but, in contrast to category II, the N-tuples containing all N different OD layers each alternate regularly the sense of their polarity in the stacking direction. Accordingly (Fig. 9.2.2.4*c*), there are two kinds of σ–ρ planes and two kinds of pairs of equivalent adjacent layers in these structures. The origin can be placed in either of the two ρ planes. c_0 is the distance between the nearest two equivalent ρ planes; a slab with this thickness contains $2 \times N$ non-equivalent OD layers. No representative of this category is known to date.

The structures of category I contain one, and only one, kind of non-polar layer, the remaining $N-1$ kinds are polar and alternate in their sense of polarity along the stacking direction (Fig. 9.2.2.4*a*). Again, there are two kinds of ρ planes here, but one is a λ–ρ plane (the layer plane of the non-polar OD layer), the other is a σ–ρ plane. These structures thus contain only one kind of pair of equivalent adjacent layers. The origin is placed in the λ–ρ plane. c_0 is the distance between the nearest two equivalent ρ planes and a slab with this thickness contains $2 \times (N-1)$ non-equivalent polar OD layers plus one entire non-polar layer. Examples are the MX_2 compounds (CdI_2, MoS_2, *etc*.) and the talc–pyrophyllite group.

The structures of category IV contain two, and only two, kinds of non-polar layers. The remaining $N-2$ kinds are polar and alternate in their sense of polarity along the stacking direction (Fig. 9.2.2.4*d*). Both kinds of ρ planes are λ–ρ planes, identical with the layer planes of the non-polar OD layers; the origin can be placed in any one of them. c_0 is chosen as in categories I and III. A slab with this thickness contains $2 \times (N-2)$ non-equivalent polar layers plus the two non-polar layers. Examples are micas, chlorites, vermiculites, *etc*.

OD structures containing $N > 1$ kinds of layers need special symbols for their OD groupoid families (Grell & Dornberger-Schiff, 1982).

A slab of thickness c_0 containing the N non-equivalent polar OD layers in the sequence as they appear in a given structure of category II represents completely its composition. In the remaining three categories, a slab with thickness $c_0/2$, the polar part of the structure contained between two adjacent ρ planes, suffices. Such slabs are higher structural units for OD structures of more than one kind of layer and have been called *OD packets*. An OD packet is thus defined as the smallest continuous part of an OD structure that is periodic in two dimensions and which represents its composition completely (Ďurovič, 1974*a*).

The hierarchy of VC structures is shown in Fig. 9.2.2.5.

9.2.2.2.8. *Desymmetrization of OD structures*

If a fully ordered structure is refined, using the space group determined from the systematic absences in its diffraction pattern and then by using some of its subgroups, serious discrepancies are only rarely encountered. Space groups thus characterize the general symmetry pattern quite well, even in real crystals. However, experience with refined periodic polytypic structures has revealed that there are always significant deviations from the OD symmetry and, moreover, even the atomic coordinates within OD layers in different polytypes of the same family may differ from one another. The OD symmetry thus appears as only an approximation to the actual symmetry pattern of polytypes. This phenomenon was called *desymmetrization* of OD structures (Ďurovič, 1974*b*, 1979).

When trying to understand this phenomenon, let us recall the structure of rock salt. Its symmetry $Fm\bar{3}m$ is an expression of the energetically most favourable relative position of Na^+ and Cl^- ions in this structure – the right angles $\alpha\beta\gamma$ follow from the symmetry. Since the whole structure is cubic, we cannot expect that the environment of any building unit, *e.g.* of any octahedron $NaCl_6$, would exercise on it an influence that would decrease its symmetry; the symmetries of these units and of the whole structure are not 'antagonistic'.

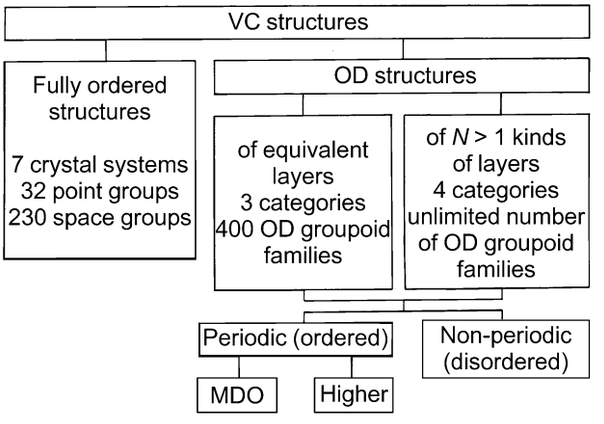

Fig. 9.2.2.5. Hierarchy of VC structures indicating the position of OD structures within it.

Not so in OD structures, where any OD layer is by definition situated in a disturbing environment because its symmetry does not conform to that of the entire structure. 'Antagonistic' relations between these symmetries are most drastic in pure MDO structures because of the regular sequence of layers. The partial symmetry operations become irrelevant and the OD groupoid degenerates into the corresponding space group.

The more disordered an OD structure is, the smaller become the disturbing effects that the environment exercises on an OD layer. These can be, at least statistically, neutralized by random positions of neighbouring layers so that partial symmetry operations can retain their relevance throughout the structure. This can be expressed in the form of a paradox: the less periodic an OD structure is, the more symmetric it appears.

Despite desymmetrization, the OD theory remains a geometrical theory that can handle properly the *general symmetry pattern* of polytypes (which group theory cannot). It establishes a *symmetry norm* with which deviations observed in real polytypes can be compared. Owing to the high abstraction power of OD considerations, systematics of entire families of polytypes at various degree-of-idealization levels can be worked out, yielding thus a common point of view for their treatment.

9.2.2.2.9. *Concluding remarks*

Although very general physical principles (OD philosophy, MDO philosophy) underlie the OD theory, it is mainly a geometrical theory, suitable for a *description* of the symmetry of polytypes and their families rather than for an *explanation* of polytypism. It thus does not compete with crystal chemistry, but cooperates with it, in analogy with traditional crystallography, where group theory does not compete with crystal chemistry.

When speaking of polytypes, one should always be aware, whether one has in mind a concrete *real* polytype – more or less in Baumhauer's sense – or an *abstract* polytype as a structural type (Subsection 9.2.2.1).

A substance can, in general, exist in the form of various polymorphs and/or polytypes of one or several families. Since polytypes of the same family differ only slightly in their crystal energy (Verma & Krishna, 1966), an entire family can be considered as an energetic analogue to one polymorph. As a rule, polytypes belonging to different families of the same substance do not co-exist. $Al(OH)_3$ may serve as an example for two different families: the bayerite family, in which the adjacent planes of OH groups are stacked according to the principle of close packing (Zvyagin *et al.*, 1979), and the gibbsite–nordstrandite family in which these groups coincide in the normal projection.* Another example is the phyllosilicates (§9.2.2.3.1). The compound $Hg_3S_2Cl_2$, on the other hand, is known to yield two polymorphs α and β (Carlson, 1967; Frueh & Gray, 1968) and one OD family of γ structures (Ďurovič, 1968).

As far as the definition of *layer polytypism* is concerned, OD theory can contribute specifications about the layers themselves and the geometrical rules for their stacking within a family (all incorporated in the vicinity condition). A possible definition might then read:

Polytypism is a special case of polymorphism, such that the individual polymorphs (called *polytypes*) may be regarded as arising through different modes of stacking layer-like structural units. The layers and their stackings are limited by the *vicinity condition*. All polytypes built on the same structural principle belong to a *family*; this depends on the degree of a structural and/or compositional *idealization*.

Geometrical theories concerning rod and block polytypism have not yet been elaborated, the main reason is the difficulty of formulating properly the vicinity condition (Sedlacek, Grell & Dornberger-Schiff, private communications). But such structures are known. Examples are the structures of tobermorite (Hamid, 1981) and of manganese(III) hydrogenbis(orthophosphite) dihydrate (Císařová, Novák & Petříček, 1982). Both structures can be thought of as consisting of a three-dimensionally periodic framework of certain atoms into which one-dimensionally periodic chains and aperiodic finite configurations of the remaining atoms, respectively, 'fit' in two equivalent ways.

9.2.2.3. *Examples of some polytypic structures*

The three examples below illustrate the three main methods of analysis of polytypism indicated in §9.2.2.2.5.

9.2.2.3.1. *Hydrous phyllosilicates*

The basic concepts were introduced by Pauling (1930*a*,*b*) and confirmed later by the determination of concrete crystal structures. A *crystallochemical analysis* of these became the basis for generalizations and systemizations. The aim was the understanding of geometrical reasons for the polytypism of these substances as well as the development of identification routines through the derivation of basic polytypes (§9.2.2.2.3). Smith & Yoder (1956) succeeded first in deriving the six basic polytypes in the mica family.

Since the 1950's, two main schools have developed: in the USA, represented mainly by Brindley, Bailey, and their co-workers (for details and references see Bailey, 1980, 1988*a*; Brindley, 1980), and in the former USSR, represented by Zvyagin and his co-workers (for details and references see Zvyagin, 1964, 1967; Zvyagin *et al.*, 1979). Both these schools based their systemizations on idealized structural models corresponding to the ideas of Pauling, with *hexagonal* symmetry of tetrahedral sheets (see later). The US school uses indicative symbols (Guinier *et al.*, 1984) for the designation of individual polytypes, and single-crystal as well as powder X-ray diffraction methods for their identification, whereas the USSR school uses unitary descriptive symbols for polytypes of all mineral groups and mainly electron diffraction on oblique textures for identification purposes. For the derivation of basic polytypes, both schools use crystallochemical considerations; symmetry principles are applied tacitly rather than explicitly.

In contrast to crystal structures based on close packings, where all relevant details of individual (even multilayer) polytypes can be recognized in the $(11\bar{2}0)$ section, the structures of hydrous phyllosilicates are rather complex. For their representation, Figueiredo (1979) used the concept of *condensed models*.

Since 1970, the OD school has also made its contribution. In a series of articles, basic types of hydrous phyllosilicates have been interpreted as OD structures of $N > 1$ kinds of layers: the serpentine–kaolin group (Dornberger-Schiff & Ďurovič, 1975*a*,*b*), Mg-vermiculite (Weiss & Ďurovič, 1980), the mica group (Dornberger-Schiff, Backhaus & Ďurovič, 1982; Backhaus & Ďurovič, 1984; Ďurovič, Weiss & Backhaus, 1984; Weiss & Wiewióra, 1986), the talc–pyrophyllite group (Ďurovič & Weiss, 1983; Weiss & Ďurovič, 1985*a*), and the chlorite group (Ďurovič, Dornberger-Schiff & Weiss, 1983;

* Sandwiches with composition $Al(OH)_3$ (similar to those in CdI_2) are the same in both families, but their stacking mode is different. This and similar situations in other substances might have been the reason for distinguishing between 'polytype diversity' and 'OD diversity' (Zvyagin, 1988).

Weiss & Ďurovič, 1983). The papers published before 1983 use the Pauling model; the later papers are based on the model of Radoslovich (1961) with *trigonal* symmetry of tetrahedral sheets. In all cases, MDO polytypes (§9.2.2.2.3) have been derived systematically: their sets partially overlap with basic polytypes presented by the US or the USSR schools. The OD models allowed the use of unitary descriptive symbols for individual polytypes from which all the relevant symmetries can be determined (Ďurovič & Dornberger-Schiff, 1981) as well as of extended indicative Ramsdell symbols (Weiss & Ďurovič, 1985*b*). The results, including principles for identification of polytypes, have been summarized by Ďurovič (1981).

The main features of polytypes of basic types of hydrous phyllosilicates, of their diffraction patterns and principles for their identification, are given in the following.

9.2.2.3.1.1. *General geometry*

Tetrahedral and octahedral sheets are the fundamental, *two-dimensionally periodic* structural units, common to all hydrous phyllosilicates. Any *tetrahedral sheet* consists of $(Si,Al,Fe^{3+},Ti^{4+})O_4$ tetrahedra joined by their three basal O atoms to form a network with symmetry $P(3)1m$ (Fig. 9.2.2.6*a*). The atomic coordinates can be related either to a hexagonal axial system with a primitive unit mesh and basis vectors $\mathbf{a}_1$, $\mathbf{a}_2$, or to an orthohexagonal system with a *c*-centred unit mesh and basis vectors $\mathbf{a}$, $\mathbf{b}$ ($b = \sqrt{3}a$). Any *octahedral sheet* consists of $M(O,OH)_6$ octahedra with shared edges (Fig. 9.2.2.6*b*), and with cations *M* most frequently Mg^{2+}, Al^{3+}, Fe^{2+}, Fe^{3+}, but also Li^+, Mn^{2+} ($r_M <\sim 0.9$ Å), *etc*. There are three octahedral sites per unit mesh $\mathbf{a}_1, \mathbf{a}_2$. Crystallochemical classification distinguishes between two extreme cases: *trioctahedral* (all three octahedral sites are occupied) and *dioctahedral* (one site is – even statistically – empty). This classification is based on a bulk chemical composition. A classification from the symmetry point of view distinguishes between three cases: *homo-octahedral* [all three octahedral sites are occupied by the same kind of crystallochemical entity, *i.e.* either by the same kind of ion or by a statistical average of different kinds of ions including voids; symmetry of such a sheet is $H(\bar{3}12/m)$;* *meso-octahedral* [two octahedral sites are occupied by the same kind of crystallochemical entity, the third by a different one, in an ordered way; symmetry $P(\bar{3}12/m)$]; and *hetero-octahedral* [each octahedral site is occupied by a different crystallochemical entity in an ordered way; symmetry $P(3)12$]. The prefixes homo-, meso-, hetero- can be combined with the prefixes tri-, di-, or used alone (Ďurovič, 1994).

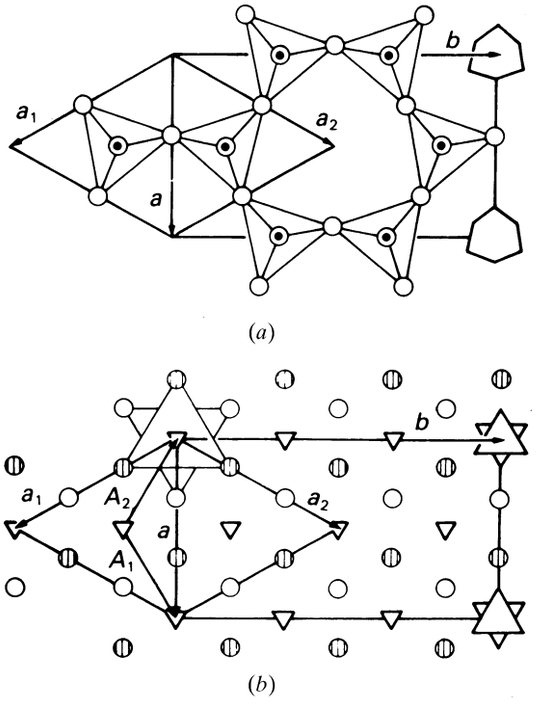

Fig. 9.2.2.6. (*a*) Tetrahedral sheet in a normal projection. Open circles: basal oxygen atoms, circles with black dots: apical oxygen atoms and tetrahedral cations. Hexagonal and orthohexagonal basis vectors and symbolic figures (ditrigons) for pictorial representation of these sheets are also shown. (*b*) Octahedral sheet. Open and shaded circles belong to the lower and the upper oxygen atomic planes, respectively; small triangles denote octahedral sites. Triangular stars on the right are the symbolic figures for pictorial representation of these sheets: the two triangles correspond to the lower and upper basis of any octahedron, respectively.

A tetrahedral sheet (*Tet*) can be combined with an octahedral sheet (*Oc*) either by a shared plane of apical O atoms (in all groups of hydrous phyllosilicates, Fig. 9.2.2.7*a*), or by hydrogen bonds (in the serpentine–kaolin group and in the chlorite group, Fig.9.2.2.7*b*). Two tetrahedral sheets can either form a pair anchored by interlayer cations (in the mica group, Fig. 9.2.2.8*a*) or an unanchored pair (in the talc–pyrophyllite group, Fig. 9.2.2.8*b*).

The ambiguity in the stacking occurs at the centres between adjacent *Tet* and *Oc* and between adjacent *Tet* in the talc–pyrophyllite group. From the solved and refined crystal structures it follows that the displacement of (the origin of) one sheet relative to (the origin of) the adjacent one can only be one (or simultaneously three – for homo-octahedral sheets) of the nine vectors shown in Fig. 9.2.2.9.

The number of possible positions of one sheet relative to the adjacent one can be determined by the corresponding *NFZ* relations (§9.2.2.2.1). As an example, the contact (*Tet*; *Oc*) by shared apical O atoms, and the contacts (*Oc*; *Tet*) by hydrogen

* A hexagonally centred unit mesh $\mathbf{a}_1, \mathbf{a}_2$ instead of a primitive mesh $\mathbf{A}_1, \mathbf{A}_2$ is used (Fig. 9.2.2.6*b*).

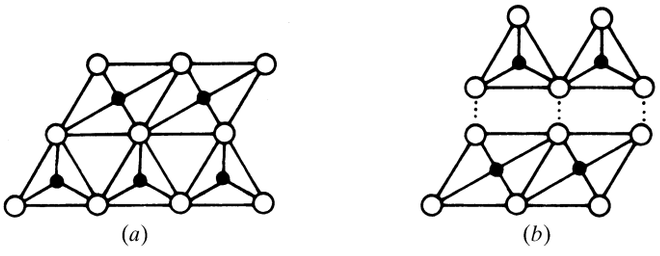

Fig. 9.2.2.7. Two possible combinations of one tetrahedral and one octahedral sheet (*a*) by shared apical O atoms, (*b*) by hydrogen bonds (side projection).

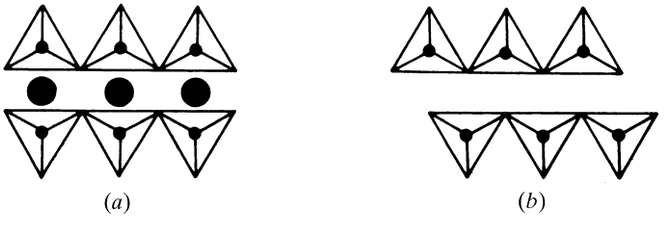

Fig. 9.2.2.8. Combination of two adjacent tetrahedral sheets (*a*) in the mica group, (*b*) in the talc–pyrophyllite group (side projection).

bonds, for a homo-octahedral case, are illustrated in Figs. 9.2.2.10(*a*) and 9.2.2.10(*b*),(*c*), respectively. The two kinds of sheets are represented by the corresponding symbolic figures indicated in Fig. 9.2.2.6. For Fig. 9.2.2.10(*a*): the symmetry of *Tet* is $P(3)1m$, thus $N = 6$; the symmetry of *Oc* is $H(\bar{3})12/m$ and its position relative to *Tet* is such that the symmetry of the pair is $P(3)1m$, thus $F = 6$ and $Z = 1$: this stacking is unambiguous.* But, if the sequence of these two sheets is reversed, $Z = 3$, because $N_{Oc} = 18$ (*h* centring of *Oc*). For Figs. 9.2.2.10(*b*) and (*c*), $Z = 3$. Similar relations can be derived for meso- and hetero-octahedral sheets as well as for the pair (*Tet*; *Tet*) in the talc–pyrophyllite group.

A detailed geometrical analysis shows that the possible positions are always related by vectors $\pm\mathbf{b}/3$. This, together with the trigonal symmetry of the individual sheets, leads to the fact that any superposition structure (§9.2.2.2.5) is trigonal (also rhombohedral) or hexagonal, and the set of diffractions with $k_{\rm ort} \equiv 0 \pmod 3$ has this symmetry too. This is important for the analysis of diffraction patterns.

Some characteristic features of basic types of hydrous phyllosilicates are as follows:

The serpentine–kaolin group: The general structural principle is shown in Fig. 9.2.2.11. The structures belong to category II (§9.2.2.2.7.2). In the homo-octahedral family, there are 12 non-equivalent (16 non-congruent) MDO polytypes (any two polytypes belonging to an enantiomorphous pair are equivalent but not congruent); in the meso-octahedral family, there are 36 non-equivalent (52 non-congruent) MDO polytypes. These sets are identical with the sets of *standard* or *regular* polytypes derived by Bailey (for references see Bailey, 1980) (trioctahedral) and by Zvyagin (1967) (dioctahedral and trioctahedral). The individual polytypes can be ranged into four groups (subfamilies, which are individual OD groupoid families), each with a characteristic superposition structure.

The mica group: The general structural principle is shown in Fig. 9.2.2.12. The structures belong to category IV. There are 6 non-equivalent (8 non-congruent) homo-octahedral MDO polytypes, 14 (22) meso-octahedral, and 36 (60) hetero-octahedral MDO polytypes. The homo-octahedral MDO polytypes are identical with those derived by Smith & Yoder (1956); meso-octahedral MDO polytypes include also those with non-centrosymmetric 2:1 layers (*Tet*; *Oc*; *Tet*); some of these have also been derived by Zvyagin *et al.* (1979). The individual polytypes can be ranged into two groups (subfamilies). For complex polytypes and growth mechanisms, see Baronnet (1975, 1986).

The talc–pyrophyllite group: The general structural principle is shown in Fig. 9.2.2.13. The structures belong to category I. There are 10 (12) MDO polytypes in the talc family (homo-octahedral) and 22 (30) MDO polytypes in the pyrophyllite family (meso-octahedral); some of these have been derived also by Zvyagin *et al.* (1979). The structures can be ranged into two

* If the symmetry of *Tet* is $P(6)mm$ (in the Pauling model), $Z = 2$. This case is common in the literature. However, with the trigonal symmetry of *Tet*, these two possibilities would correspond to Franzini (1969) types *A* and *B*, which are not geometrically equivalent.

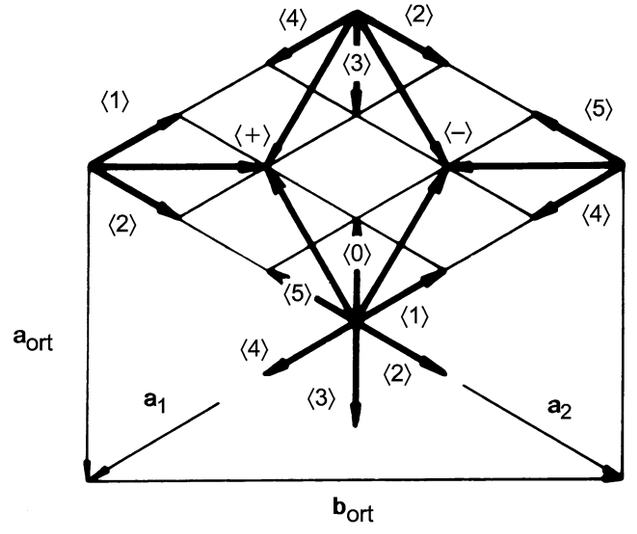

Fig. 9.2.2.9. The nine possible displacements in the structures of polytypes of phyllosilicates. The individual vectors are designated by their conventional numerical characters and the signs +,−. The zero displacement ⟨∗⟩ is not indicated. The relations of these vectors to the basis vectors $\mathbf{a}_1, \mathbf{a}_2$ or $\mathbf{a}, \mathbf{b}$ are evident.

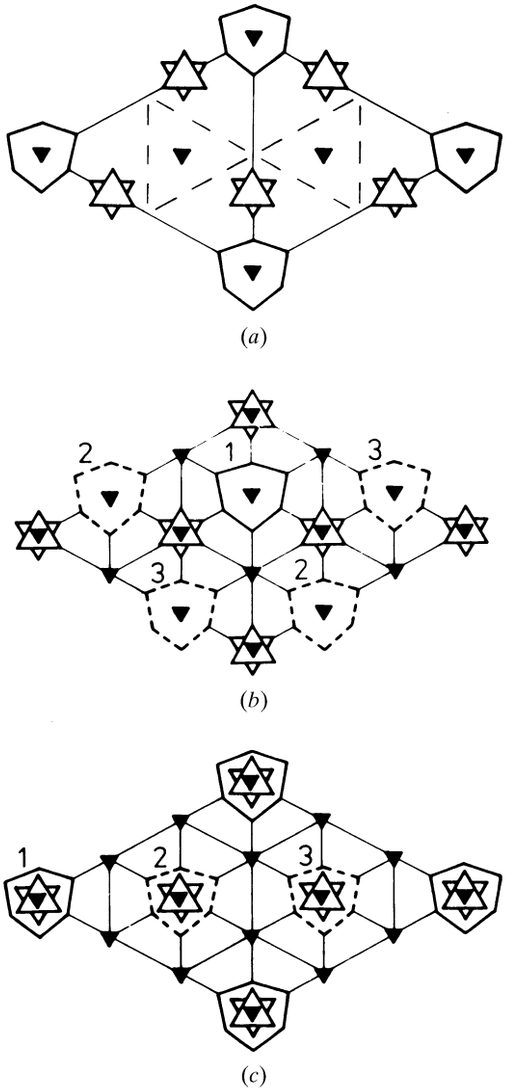

Fig. 9.2.2.10. The *NFZ* relations (*a*) for the pair tetrahedral sheet–homo-octahedral sheet (with shared apical O atoms), (*b*), (*c*) for the pair homo-octahedral sheet–tetrahedral sheet (by hydrogen bonds). The sheets are represented by their symbolic figures; some relevant symmetry elements are also indicated. One of the possible positions (labelled 1) is drawn by full, the other two (2, 3) by broken lines.

groups (subfamilies). For more details, see also Evans & Guggenheim (1988).

The chlorite–vermiculite group: There are two kinds of octahedral sheets in these structures: the *Oc* sandwiched between two *Tet* and the *interlayer* (Fig. 9.2.2.14). The structures belong to category IV. Any *Oc* can be independently homo-, meso-, or hetero-octahedral, and thus, theoretically, there are nine families here. Although vermiculites have a crystal chemistry different from chlorites, they can be, from the symmetry point of view, treated together. There are 20 (24) homo-homo-octahedral, 44 (60) homo-meso-octahedral and 164 (256) meso-meso-octahedral MDO polytypes (the first prefix refers to the 2:1 layer, the second to the interlayer); the other families have not yet been treated. Some of these polytypes have also been derived by other authors (for references, see Bailey, 1980; Zvyagin *et al.*, 1979).

In order to preserve a unitary system, some monoclinic polytypes necessitate a 'third' setting, with the *a* axis unique. These should not be transformed into the standard second setting.

9.2.2.3.1.2. *Diffraction pattern and identification of individual polytypes*

Owing to the trigonal symmetry of the basic structural units and their stacking mode, the single-crystal diffraction pattern of hydrous phyllosilicates has a hexagonal *geometry* and it can be referred to hexagonal or orthohexagonal reciprocal vectors $\mathbf{a}_1^*$, $\mathbf{a}_2^*$ or $\mathbf{a}^*$, $\mathbf{b}^*$, respectively (Figs. 9.2.2.15 and 9.2.2.16). It contains three types of diffractions:

(1) Diffractions 00*l* (or 000*l*), always sharp and common to all polytypes of a family including all its subfamilies. They are indicative of the mineral group, but useless for the identification of polytypes.

(2) The remaining diffractions with $k_{\rm ort} \equiv 0 \pmod 3$, always sharp and common to all polytypes of the same subfamily.

(3) All other diffractions: sharp only for periodic polytypes, otherwise present on diffuse rods parallel to $\mathbf{c}^*$. These are characteristic of individual polytypes. Diffractions 0*kl* – if sharp – are common to all polytypes of the family with the same *bc* projection.

From descriptive geometry, it is known that two orthogonal projections suffice to characterize unambiguously any structure and, therefore, the superposition structure (which implicitly contains the *ac* projection) together with the *bc* projection suffice for an unambiguous characterization of any polytype. It also follows that the diffractions with $k \equiv 0 \pmod 3$ together with the 0*kl* diffractions with $k \not\equiv 0 \pmod 3$ suffice for its determination (except for homometric structures) (Ďurovič, 1981).

From the trigonal or hexagonal symmetry of any superposition structure and from Friedel's law, it follows that the reciprocal rows 20*l*, 13*l*, $\bar{1}3l$, $\bar{2}0l$, $\bar{1}\bar{3}l$, and $1\bar{3}l$ (Fig. 9.2.2.16) carry the same information. Therefore, for identification purposes, it suffices to calculate the distribution of intensities along the reciprocal rows 20*l* (superposition structure – subfamily) and 02*l* (*bc* projection) for all MDO polytypes. Experience shows (Weiss & Ďurovič, 1980) that a mere visual comparison of calculated and observed intensities along these two rows suffices for an unambiguous identification of a MDO polytype. A similar scheme has been presented by Bailey (1988*b*).

The above considerations are based on the ideal Radoslovich model. Diffraction patterns of real structures may exhibit deviations owing to the distortion of the ideal lattice geometry and/or symmetry of the structure.

9.2.2.3.2. *Stibivanite Sb_2VO_5*

The crystal structure of this mineral has been determined by Szymański (1980). It turned out to be identical with that of the compound of the same composition synthesized earlier (Darriet, Bovin & Galy, 1976). The structure is monoclinic with space group $C12/c1$, lattice parameters $a = 17.989\ (6)$, $b = 4.7924\ (7)$, $c = 5.500\ (2)$ Å, $\beta = 95.13\ (3)^\circ$.

Structural units are formed of SbO_2–O–VO–O–SbO_2 extended along **a**, with adjacent units bonded along **c** through Sb—O—Sb and V—O—V bonds. Ribbons are thus formed with no bonding along **b**, and only the Sb—O interactions [2.561 (4) Å] along **a** (Fig. 9.2.2.17). This accounts for the excellent acicular cleavage.

Merlino *et al.* (1989) recognized in this structure sheets of VO_5 square pyramids (*Pyr*) parallel to **bc**, with layer symmetry $P(2/m)2/c2_1/m$ alternating with sheets containing chains of distorted SbO_3 tetrahedron-like pyramids (*Tet*) with layer symmetry $P(1)2_1/c1$ (Fig. 9.2.2.18). Owing to the higher symmetry of *Pyr*, they concluded that there may also exist an alternative attachment of *Tet* to *Pyr*, such that the triples (*Tet*; *Pyr*; *Tet*) will exhibit the layer symmetry $Pmc2_1$, and they will be arranged so that another polytype 2*O* with symmetry $P2_1/m2_1/c2_1/n$ (Fig. 9.2.2.19) is formed [in the original 2*M* polytype, the triples (*Tet*; *Pyr*; *Tet*) have the layer symmetry $P(1)2/c1$]. A mineral with such a structure, with lattice parameters $a = 17.916\ (3)$, $b = 4.700\ (1)$, $c = 5.509\ (1)$ Å, has actually been found.

The polytypism of stibivanite is reflected in its OD character: the two kinds of sheets *Pyr* and *Tet* correspond to two kinds of non-polar layers: their relative position is given by the family symbol:

$$\begin{array}{ll} P(1)2_1/c1 & P(m)cm \\ [1/4, -0.0733\ldots] & \text{category IV,} \end{array}$$

the *NFZ* relations being

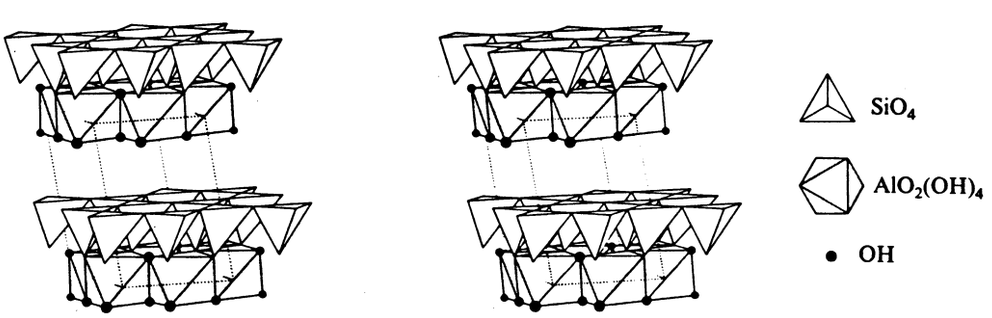

Fig. 9.2.2.11. Stereopair showing the sequence of sheets in the structures of the serpentine–kaolin group (kaolinite-1*A*, courtesy Zoltai & Stout, 1985).

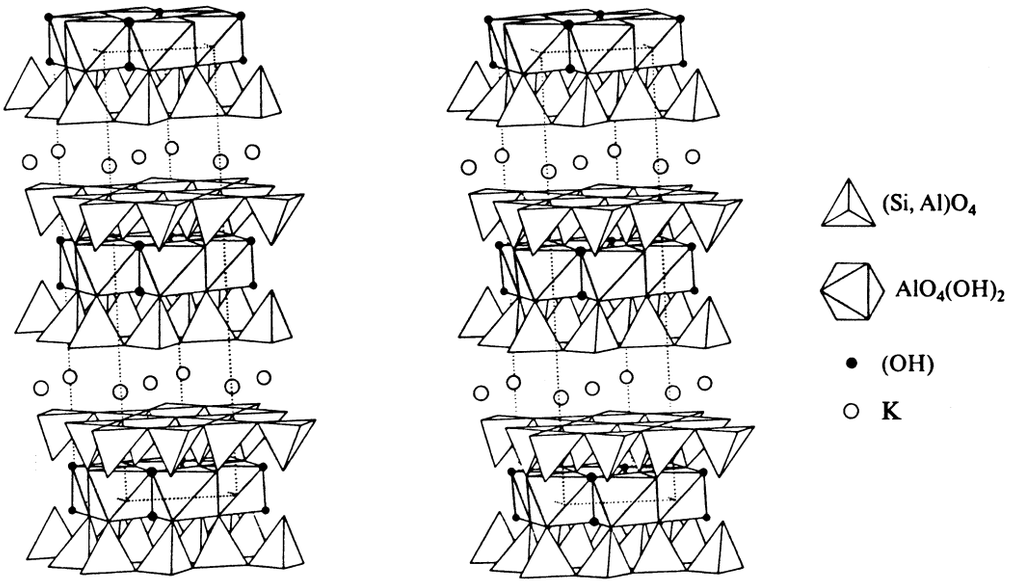

Fig. 9.2.2.12. Stereopair showing the sequence of sheets in the structures of the mica group (muscovite-2M_1, courtesy of Zoltai & Stout, 1985).

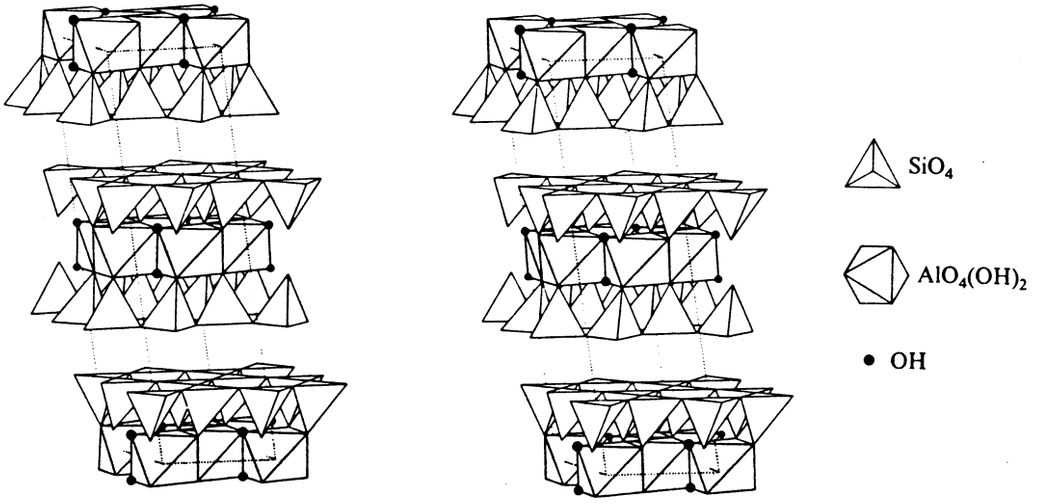

Fig. 9.2.2.13. Stereopair showing the sequence of sheets in the structures of the talc-pyrophyllite group (pyrophyllite-2M, courtesy of Zoltai & Stout, 1985).

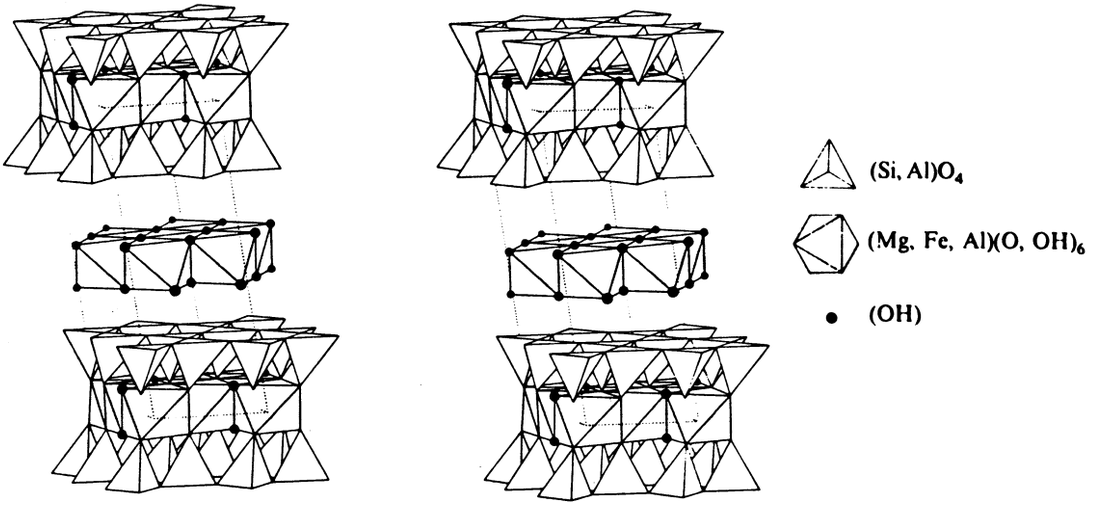

Fig. 9.2.2.14. Stereopair showing the sequence of sheets in the structures of the chlorite–vermiculite group (chlorite-1M, courtesy of Zoltai & Stout, 1985).

OD layer	layer group	subgroup of λ–τ oper.	N	F	Z
L_{2n+1}	$P(2/m)\,2/c\,2_1/m$	$P(2)cm$	4		1
			↘		↗
				2	
			↗		↘
L_{2n}	$P(1)\,2_1/c\,1$	$P(1)c1$	2		2.

Both polytypes are slightly desymmetrized. Since the shift between the origins of *Pyr* and *Tet* is irrational, stibivanite has no superposition structure and thus the diffraction patterns of its polytypes have no common set of family diffractions. Another remarkable point is that the recognition of these structures as OD structures of *layers* has nothing to do with their system of chemical bonds (see above).

9.2.2.3.3. γ-$Hg_3S_2Cl_2$

Among about 40 investigated crystals synthesized by Carlson (1967), not one was periodic. All diffraction patterns exhibited a common set of family diffractions, but the distribution of intensities along diffuse streaks varied from crystal to crystal (Ďurovič, 1968). The maxima on these streaks indicated in some cases a simultaneous presence of domains of three periodic polytypes – one system of diffuse maxima was always present and it was referred to a rectangular cell with $a = 9,328\,(5)$, $b = 16.28\,(1)$, $c = 9.081\,(6)$ Å with monoclinic symmetry. All crystals were more or less twinned, sometimes simulating orthorhombic symmetry in their diffraction patterns.

The superposition structure with $\mathbf{A} = \mathbf{a}$, $\mathbf{B} = \mathbf{b}/2$, $\mathbf{C} = 2\mathbf{c}$ and space group *Pbmm* was solved first. Here, a comparison of the family diffractions with the diffraction pattern of the α modification (Frueh & Gray, 1968) proved decisive. It turned out that only one kind of Hg atom contributed with half weight to the superposition structure. This means that only these atoms repeat in the actual structure with periods $\mathbf{b} = 2\mathbf{B}$ and $\mathbf{c} = 2\mathbf{C}$. All other atoms (in the first approximation) repeat with the periods of the superposition structure and thus do not contribute to the diffuse streaks.

The symmetry of the superposition structures is compatible with the OD groupoid family determined from systematic absences:

$A(2)$	m	m	
$\{(b_{1/2})$	$2_{1/2}$	$2\}$	
$\{(b_{1/2})$	$2_{1/2}$	$2\}$	category III,

where the subscripts 1/2 indicate translational components of $b/4$ (Dornberger-Schiff, 1964, pp. 41 ff.).

The solution of the structural principle thus necessitated only the correct location of the 'disordered' Hg atom in one of two

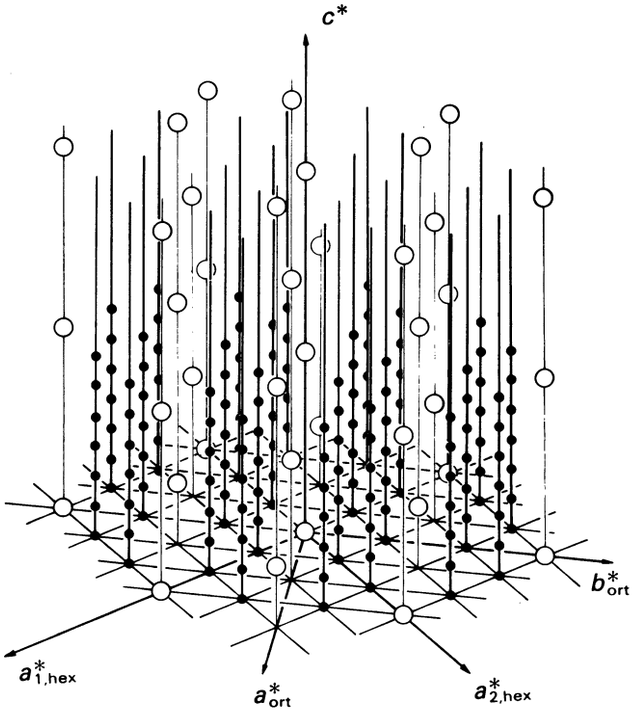

Fig. 9.2.2.15. Clinographic projection of the general scheme of a single-crystal diffraction pattern of hydrous phyllosilicates. Family diffractions are indicated by open circles and correspond in this case to a rhombohedral superposition structure. Only the part with $l \geq 0$ is shown.

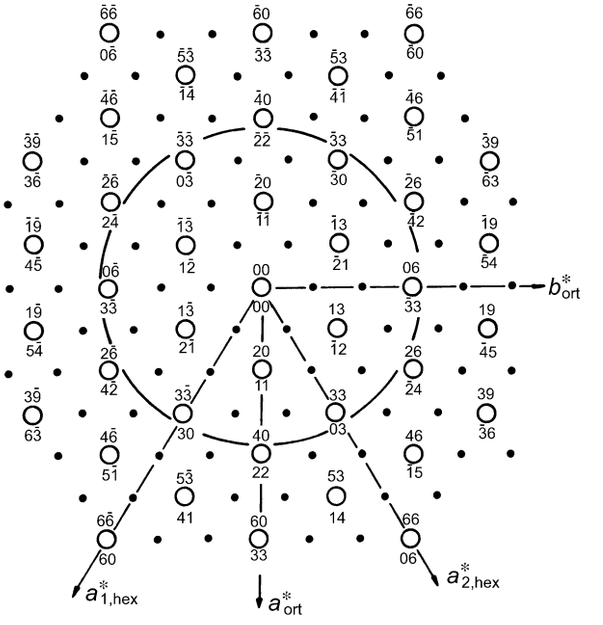

Fig. 9.2.2.16. Normal projection of the general scheme of a single-crystal diffraction pattern of hydrous phyllosilicates. Rows of family diffractions are indicated by open circles; the h, k indices refer to hexagonal (below) and orthogonal (above) axial systems.

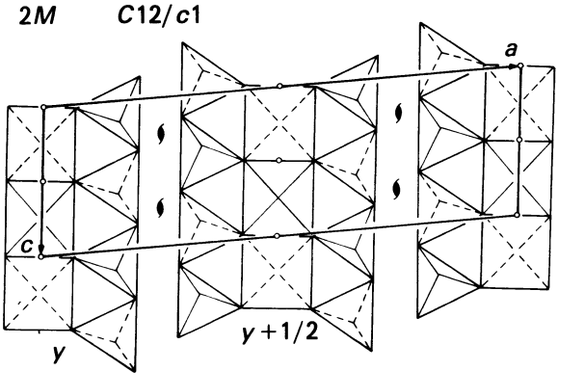

Fig. 9.2.2.17. The structure of stibivanite-2M. The unit cell is outlined and some relevant symmetry operations are indicated (after Merlino *et al.*, 1989).

possible positions indicated by the superposition structure. An analysis of the Fourier transform relevant to the above OD groupoid family showed that the Patterson function calculated with coefficients $|\Lambda(hkl)|^2 = |F(hkl)|^2 + |F(\bar{h}kl)|^2$ shows interatomic vectors *within* any single OD layer, and it turned out that even a first generalized projection of the function yields the necessary 'yes/no' answer.

The structural principle is shown in Fig. 9.2.2.20.

There are two MDO polytypes in this family. Both are monoclinic (*c* axis unique) and consist of equivalent triples of OD layers. The first, MDO_1, is periodic after two layers and has symmetry $A2/m$. The second, MDO_2, is periodic after four layers, has symmetry $F2/m$ and basis vectors $2\mathbf{a}, \mathbf{b}, \mathbf{c}$. Domains of MDO_1 were present in all crystals (the system of diffuse maxima, mentioned above), but some of them also contained small proportions of MDO_2.

Later, single crystals of pure periodic MDO_1 were also found in specimens prepared hydrothermally (Rabenau, private communication). The results of a structure analysis confirmed the previous results but indicated desymmetrization (Ďurovič, 1979). The atomic coordinates deviated significantly from the ideal OD model; the monoclinic angle became 90.5°. Even the family diffractions, which in the disordered crystals exhibited an orthorhombic symmetry, deviated significantly from it in their positions and intensities.

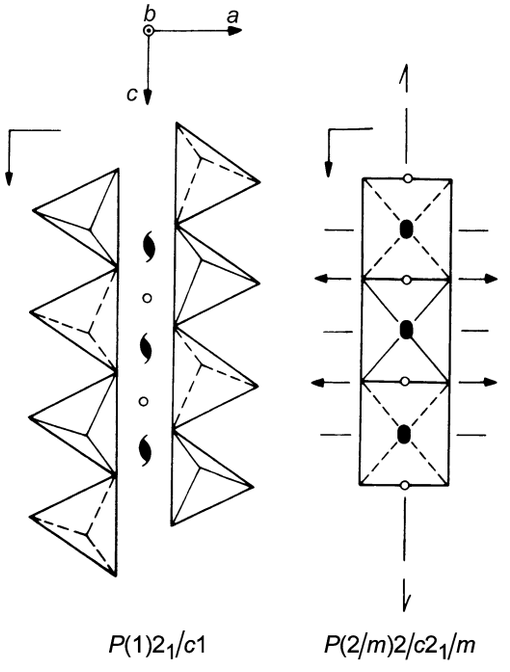

Fig. 9.2.2.18. The two kinds of OD layers in the stibivanite family (after Merlino *et al.*, 1989).

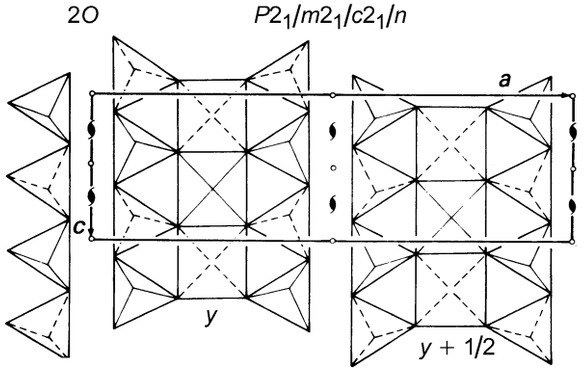

Fig. 9.2.2.19. The structure of stibivanite-2*O* (after Merlino *et al.*, 1989).

9.2.2.3.4. *Remarks for authors*

When encountering a polytypic substance showing disorder, many investigators try to find in their specimens a periodic single crystal suitable for a structure analysis by current methods. So far, no objections. But a common failing is that they often neglect to publish a detailed account of the disorder phenomena observed on their diffraction photographs: presence or absence of diffuse streaks, their position in reciprocal space, positions of diffuse maxima, suspicious twinning, non-space-group absences, higher symmetry of certain subsets of diffractions, *etc*. These data should always be published, even if the author does not interpret them: otherwise they will inevitably be lost. Similarly, preliminary diffraction photographs (even of poor quality) showing these phenomena and the crystals themselves should be preserved – they may be useful for someone in the future.

9.2.2.4. *List of some polytypic structures*

A few examples of some less-common polytypic structures published up to 1994 are listed below:

Minerals: McGillite (Iijima, 1982), tridymite (Wennemer & Thompson, 1984), pyrosmalite (Takéuchi, Ozawa & Takahata, 1983), zirconolite (White, Segall, Hutchison & Barry, 1984), Ti-biotite (Zhukhlistov, Zvyagin & Pavlishin, 1990), diamond (Phelps, Howard & Smith, 1993), scholzite (Taxer, 1992), fiedlerite (Merlino, Pasero & Perchiazzi, 1994), penkvilskite (Merlino, Pasero, Artioli & Khomyakov, 1994), lengebachite – non-commensurate structure (Makovický, Leonardsen & Moelo, 1994).

Inorganic compounds: Borates with general formula $RAl_3(BO_3)_4$, where R = Y, Nd, Gd (Belokoneva & Timchenko,

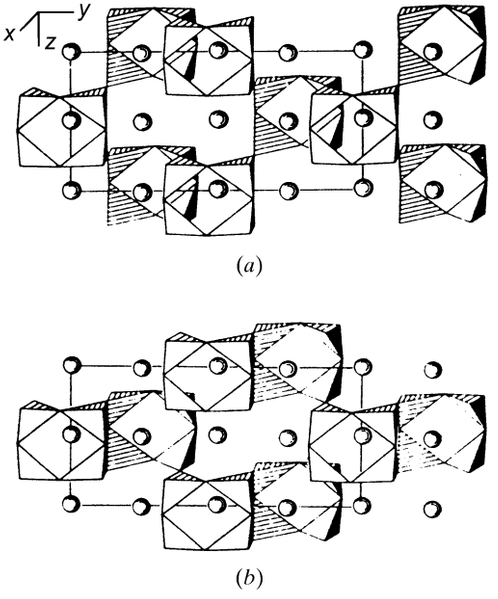

Fig. 9.2.2.20. The structural principle of γ-$Hg_3S_2Cl_2$. The shared corners of the pyramids are occupied by the Hg atoms; unshared corners are occupied by the S atoms. A pair of layers, but only the Cl atoms at their common boundary, are drawn. The two geometrically equivalent arrangements (*a*) and (*b*) are shown.

1983), $BaCrO_3$ (Chamberland, 1983), hexacyanocomplexes of transition metals (Jagner, 1985), chromium iron carbides (Kowalski, 1985), $Fe_{1-x}S$ (Kuban, 1985), hexagonal copper(I) ferrite (Effenberger, 1991), $PbS \cdot 18TiS_2$ – a modulated structure (van Smaalen & de Boer, 1992), α-$LiNH_4SO_4$ (Tomaszewski, 1992), fullerene C_{60} (de Boer, van Smaalen, Petříček, Dušek, Verheijen & Meijer, 1994).

Organic compounds: Oxalates (Fichtner-Schmittler, 1979), primetine (Jarchow & Schmalle, 1985), 2-hydroxy-4-methoxy-2*H*-1,4-benzoxazin-3-one, $C_9H_9NO_4$ (Kutschabsky, Kretschmer, Schrauber, Dathe & Schneider, 1986), carbamazepine dihydrate (Reck & Dietz, 1986), piroxicam (Reck, Dietz, Laban, Günther, Bannier & Höhne, 1988), *E*-octadecanoic acid (Kaneko, Sakashita, Kobayashi, Kitagawa, Matsuura & Suzuki, 1994).

Metals, intermetallic compounds and alloys: Alloys are treated in a monograph by Nikolin (1984); a lecture note by Amelinckx (1986) gives details of high-resolution electron microscopy and examples of the investigation of some alloys but also of other polytypic structures. Special papers: Li metal (Schwarz & Blaschko, 1990), $Zr(FeCr)_2$ Laves phases (Burany & Northwood, 1991), doped Co–W and Co–Mo alloys (Nikolin, Babkevich, Izdkovskaya & Petrova, 1993).

Further data are given in articles by Bailey *et al*. (1977), Dornberger-Schiff (1979), Zvyagin (1988), Baronnet (1992) and Zorkii & Nesterova (1993).

High-resolution electron microscopy (HREM) applied in the structure analysis of (also disordered) polytypic substances: orientite (Mellini, Merlino & Pasero, 1986), ardennite (Pasero & Reinecke, 1991), pseudowollastonite (Ingrin, 1993), laurionite and paralaurionite (Merlino, Pasero & Perchiazzi, 1993), perovskites in the system $La_4Ti_3O_{12}$–$LaTiO_3$ (Bontchev, Darriet, Darriet, Weill, Van Tendeloo & Amelinckx, 1993), baumhauerite (Pring & Graeser, 1994), bementite (Heinrich, Eggleton & Guggenheim, 1994), parsettensite (Eggleton & Guggenheim, 1994).

O'Keeffe, M. (1992). *Uninodal 4-connected 3D nets. II. Nets with 3-rings. Acta Cryst.* A**48**, 670–673.

O'Keeffe, M. (1998). *Sphere packings and space filling by congruent simple polyhdra. Acta Cryst.* A**54**, 320–329.

O'Keeffe, M. & Brese, N. E. (1992). *Uninodal 4-connected 3D nets. I. Nets without 3- or 4-rings. Acta Cryst.* A**48**, 663–669.

Schnering, H. G. von & Nesper, R. (1987). *Die natürliche Anpassung von chemischen Strukturen an gekrümmte Flächen. Angew. Chem.* **99**, 1097–1119.

Shubnikov, A. V. (1916). *On the structure of crystals. Izv. Akad. Nauk SSSR Ser.* 6, **10**, 755–799.

Sinogowitz, U. (1939). *Die Kreislagen und Packungen kongruenter Kreise in der Ebene. Z. Kristallogr.* **100**, 461–508.

Sinogowitz, U. (1943). *Herleitung aller homogenen nicht kubischen Kugelpackungen. Z. Kristallogr.* **105**, 23–52.

Slack, G. A. (1983). *The most-dense and least-dense packings of circles and spheres. Z. Kristallogr.* **165**, 1–22.

Smirnova, N. L. (1956*a*). *Structure types with atomic close packing: possible structure types for the composition AB_3. Sov. Phys. Crystallogr.* **1**, 128–131.

Smirnova, N. L. (1956*b*). *Structure types with closest atomic packing: possible structure types for the AB_4 composition. Sov. Phys. Crystallogr.* **1**, 399–401.

Smirnova, N. L. (1958*a*). *Structural types for close packing of atoms. III. Possible structures for the composition AB_6. Sov. Phys. Crystallogr.* **3**, 232–234.

Smirnova, N. L. (1958*b*). *On structural types with closest atomic packing. Possible structural types with the composition AB_{12}. Sov. Phys. Crystallogr.* **3**, 362–364.

Smirnova, N. L. (1959*a*). *The superstructures possible in close-packed structures. Sov. Phys. Crystallogr.* **4**, 10–16.

Smirnova, N. L. (1959*b*). *Possible superstructures in a simple cubic structure. Sov. Phys. Crystallogr.* **4**, 17–20.

Smirnova, N. L. (1959*c*). *Possible arrangement of atoms in the octahedral voids in the hexagonal close-packed structure. Sov. Phys. Crystallogr.* **4**, 734–737.

Smirnova, N. L. (1964). *Possible superstructures in the n-th layer of closest packing. B atoms have 4 or 2; or 4 or 1 nearest A atoms. Sov. Phys. Crystallogr.* **9**, 206–208.

Sowa, H. (1988). *Changes of the oxygen packing of low quartz and ReO_3-structure under high pressure. Z. Kristallogr.* **184**, 257–268.

Sowa, H. (1997). *Pressure-induced $Fm\bar{3}m \rightarrow R\bar{3}$ phase transition in $NaSbF_6$. Acta Cryst.* B**53**, 25–31.

Sowa, H. & Koch, E. (1999). *Sphere configurations with symmetry $R\bar{3}m$ 18(h).m. Z. Kristallogr. Submitted.*

Tanemura, M. & Matsumoto, T. (1992). *On the density of the p31m packing of ellipses. Z. Kristallogr.* **198**, 89–99.

Treacy, M. M. J., Randall, K. H., Rao, S., Perry, J. A. & Chadi, D. J. (1997). *Enumeration of periodic tetrahedral frameworks. Z. Kristallogr.* **212**, 768–791.

Wells, A. F. (1977). *Three-dimensional nets and polyhedra.* New York: John Wiley & Sons.

Wells, A. F. (1979). *Further studies of three-dimensional nets.* ACA Monograph No. 8.

Wells, A. F. (1983). *Six new three-dimensional 3-connected nets $4.n^2$. Acta Cryst.* B**39**, 652–654.

Zobetz, E. (1983). *Über Kugellagerungen, Wirkungsbereichsteilungen und Koordinationszahlen von Punktkonfigurationen mit trigonaler Symmetrie $R\bar{3}m$. Z. Kristallogr.* **163**, 167–180.

Adamsky, R. F. & Merz, K. M. (1959). *Synthesis and crystallography of the wurtzite form of silicon carbide. Z. Kristallogr.* **111**, 350–361.

Andrade, M., Chandrasekaran, M. & Delaey, L. (1984). *The basal plane stacking faults in 18R martensite of copper base alloys. Acta Metall.* **32**, 1809–1816.

Azaroff, L. V. (1960). *Introduction to solids.* London: McGraw-Hill.

Belov, N. V. (1947). *The structure of ionic crystals and metal phases.* Moscow: Izd. Akad. Nauk SSSR. [In Russian.]

Bertaut, E. F. (1978). *The equivalent charge concept and its application to the electrostatic energy of charges and multipoles. J. Phys. (Paris)*, **39**, 1331–1348.

Boerdijk, A. H. (1952). *Some remarks concerning close-packing of equal spheres. Philips Res. Rep.* **7**, 303–313.

Brafman, O., Alexander, E. & Steinberger, I. T. (1967). *Five new zinc sulphide polytypes: 10L(82); 14L (5423); 24L $(53)_3$; 26L (17 423) and 28L (9559). Acta Cryst.* **22**, 347–252.

Brafman, O. & Steinberger, I. T. (1966). *Optical band gap and birefringence of ZnS polytypes. Phys. Rev.* **143**, 501–505.

Buerger, M. J. (1953). *X-ray crystallography.* New York: John Wiley.

Chadha, G. K. (1977). *Identification of the rhombohedral lattice in CdI_2 crystals. Acta Cryst.* A**33**, 341.

Cottrell, A. (1967). *An introduction to metallurgy.* London: Edward Arnold.

Cowley, J. M. (1976). *Diffraction by crystals with planar faults. I. General theory. Acta Cryst.* A**32**, 83–87.

Dornberger-Schiff, K. & Farkas-Jahnke, M. (1970). *A direct method for the determination of polytype structures. I. Theoretical basis. Acta Cryst.* A**26**, 24–34.

Dubey, M. & Singh, G. (1978). *Use of lattice imaging in the electron microscope in the structure determination of the 126R polytype of SiC. Acta Cryst.* A**34**, 116–120.

Dubey, M., Singh, G. & Van Tendeloo, G. (1977). *X-ray diffraction and transmission electron microscopy study of extremely large-period polytypes in SiC. Acta Cryst.* A**33**, 276–279.

Farkas-Jahnke, M. (1983). *Structure determination of polytypes. Crystal growth and characterization of polytype structures*, edited by P. Krishna, pp. 163–211. Oxford: Pergamon Press.

Farkas-Jahnke, M. & Dornberger-Schiff, K. (1969). *A direct method for the determination of polytype structures. II. Determination of a 66R structure. Acta Cryst.* A**25**, 35–41.

Frank, F. C. (1951). *Crystal dislocation – elementary concepts and definitions. Philos. Mag.* **42**, 809–819.

Hendricks, S. & Teller, E. (1942). *X-ray interference in partially ordered layer lattices. J. Chem. Phys.* **10**, 147–167.

Honjo, G., Miyake, S. & Tomita, T. (1950). *Silicon carbide of 594 layers. Acta Cryst.* **3**, 396–397.

Jagodzinski, H. (1949*a*). *Eindimensionale Fehlordnung in Kristallen und ihr Einfluss auf die Rontgeninterferenzen. I. Berechnung des Fehlordnungsgrades aus den Rontgenintensitaten. Acta Cryst.* **2**, 201–207.

Jagodzinski, H. (1949*b*). *Eindimensionale Fehlordnung in Kristallen und ihr Einfluss auf die Rontgeninterferenzen.II. Berechnung de fehlgeordneten dichtesten Kugelpackungen mit Wechselwirkungen der Reichweite 3. Acta Cryst.* **2**, 208–214.

Jagodzinski, H. (1972). *Transition from cubic to hexagonal silicon carbide as a solid state reaction. Sov. Phys. Crystallogr.* **16**, 1081–1090.

9.2.1 (*cont.*)

Jain, P. C. & Trigunayat, G. C. (1977*a*). *On centrosymmetric space groups in close-packed MX_2-type structures*. *Acta Cryst.* A**33**, 255–256.

Jain, P. C. & Trigunayat, G. C. (1977*b*). *Resolution of ambiguities in Zhdanov notation: actual examples of homometric structures*. *Acta Cryst.* A**33**, 257–260.

Johnson, C. A. (1963). *Diffraction by FCC crystals containing extrinsic stacking faults*. *Acta Cryst.* **16**, 490–497.

Kabra, V. K. & Pandey, D. (1988). *Long range ordered phases without short range correlations*. *Phys. Rev. Lett.* **61**, 1493–1496.

Kabra, V. K., Pandey, D. & Lele, S. (1986). *On a diffraction approach for the study of the mechanism of 3C to 6H transformation in SiC*. *J. Mater. Sci.* **21**, 1654–1666.

Kabra, V. K., Pandey, D. & Lele, S. (1988*a*). *On the characterization of basal plane stacking faults in the N9R and N18R martensites*. *Acta Metall.* **36**, 725–734.

Kabra, V. K., Pandey, D. & Lele, S. (1988*b*). *On the calculation of diffracted intensities from SiC crystals undergoing 2H to 6H transformation by the layer displacement mechanism*. *J. Appl. Cryst.* **21**, 935–942.

Kakinoki, J. & Komura, Y. (1954). *Intensity of X-ray diffraction by a one-dimensionally disordered crystal. III. The close-packed structure*. *J. Phys. Soc. Jpn,* **9**, 177–183.

Krishna, P. & Marshall, R. C. (1971*a*). *The structure, perfection and annealing behaviour of SiC needles grown by a VLS mechanism*. *J. Cryst. Growth*, **9**, 319–325.

Krishna, P. & Marshall, R. C. (1971*b*). *Direct transformation from the 2H to 6H structure in single crystal SiC*. *J. Cryst. Growth*, **11**, 147–150.

Krishna, P. & Pandey, D. (1981). *Close-packed structures*. Teaching Pamphlet of the International Union of Crystallography. University College Cardiff Press.

Krishna, P. & Verma, A. R. (1962). *An X-ray diffraction study of silicon carbide structure types $[(33)_n34]_3R$*. *Z. Kristallogr.* **117**, 1–15.

Krishna, P. & Verma, A. R. (1963). *Anomalies in silicon carbide polytypes*. *Proc. R. Soc. London Ser. A*, **272**, 490–502.

Mesquita, A. H. G. de (1967). *Refinement of the crystal structure of SiC type 6H*. *Acta Cryst.* **23**, 610–617.

Mitchell, R. S. (1953). *Application of the Laue photograph to the study of polytypism and syntaxic coalescence in silicon carbide*. *Am. Mineral.* **38**, 60–67.

Nishiyama, Z. (1978). *Martensitic transformation*. New York: Academic Press.

Pandey, D. (1984*a*). *Stacking faults in close-packed structures: notations and definitions*. Deposited with the British Library Document Supply Centre as Supplementary Publication No. SUP 39176 (23 pp.). Copies may be obtained through The Managing Editor, International Union of Crystallography, 5 Abbey Square, Chester CH1 2HU, England.

Pandey, D. (1984*b*). *A geometrical notation for stacking faults in close-packed structures*. *Acta Cryst.* B**40**, 567–569.

Pandey, D. (1985). *Origin of polytype structures in CdI_2: application of faulted matrix model revisited*. *J. Cryst. Growth,* **71**, 346–352.

Pandey, D. (1988). *Role of stacking faults in solid state transformations*. *Bull. Mater. Sci.* **10**, 117–132.

Pandey, D., Kabra, V. K. & Lele, S. (1986). *Structure determination of one-dimensionally disordered polytypes*. *Bull. Minéral.* **109**, 49–67.

Pandey, D. & Krishna, P. (1975). *On the spiral growth of polytype structures in SiC from a faulted matrix. I. Polytypes based on the 6H structure*. *Mater. Sci. Eng.* **20**, 243–249.

Pandey, D. & Krishna, P. (1976*a*). *On the spiral growth of polytype structures in SiC from a faulted matrix. II. Polytypes based on the 4H and 15R structures*. *Mater. Sci. Eng.* **26**, 53–63.

Pandey, D. & Krishna, P. (1976*b*). *X-ray diffraction from a 6H structure containing intrinsic faults*. *Acta Cryst.* A**32**, 488–492.

Pandey, D. & Krishna, P. (1977). *X-ray diffraction study of stacking faults in single crystal of 2H SiC*. *J. Phys. D*, **10**, 2057–2068.

Pandey, D. & Krishna, P. (1982*a*). *Polytypism in close-packed structures*. *Current topics in materials science,* Vol. IX, edited by E. Kaldis, pp. 415–491. Amsterdam: North-Holland.

Pandey, D. & Krishna, P. (1982*b*). *X-ray diffraction study of periodic and random faulting in close-packed structures*. *Synthesis, crystal growth and characterization of materials*, edited by K. Lal, pp. 261–285. Amsterdam: North-Holland.

Pandey, D. & Krishna, P. (1983). *The origin of polytype structures*. *Crystal growth and characterization of polytype structures*, edited by P. Krishna, pp. 213–257. Oxford: Pergamon Press.

Pandey, D. & Lele, S. (1986*a*). *On the study of the FCC–HCP martensitic transformation using a diffraction approach. I. FCC→HCP transformation*. *Acta Metall.* **34**, 405–413.

Pandey, D. & Lele, S. (1986*b*). *On the study of the FCC–HCP martensitic transformation using a diffraction approach. II. HCP→FCC transformation*. *Acta Metall.* **34**, 415–424.

Pandey, D., Lele, S. & Krishna, P. (1980*a*). *X-ray diffraction from one-dimensionally disordered 2H crystals undergoing solid state transformation to the 6H structure. I. The layer displacement mechanism*. *Proc. R. Soc. London Ser. A*, **369**, 435–449.

Pandey, D., Lele, S. & Krishna, P. (1980*b*). *X-ray diffraction from one-dimensionally disordered 2H crystals undergoing solid state transformation to the 6H structure. II. The deformation mechanism*. *Proc. R. Soc. London Ser. A*, **369**, 451–461.

Pandey, D., Lele, S. & Krishna, P. (1980*c*). *X-ray diffraction from one-dimensionally disordered 2H crystals undergoing solid state transformation to the 6H structure. III. Comparison with experimental observations on SiC*. *Proc. R. Soc. London Ser. A*, **369**, 463–477.

Pandey, D., Prasad, L., Lele, S. & Gauthier, J. P. (1987). *Measurement of the intensity of directionally diffuse streaks on a 4-circle diffractometer: divergence correction factors for bisecting setting*. *J. Appl. Cryst.* **20**, 84–89.

Paterson, M. S. (1952). *X-ray diffraction by face-centred cubic crystals with deformation faults*. *J. Appl. Phys.* **23**, 805–811.

Patterson, A. L. & Kasper, J. S. (1959). *Close-packing*. *International tables for X-ray crystallography*, Vol. II, edited by J. S. Kasper & K. Lonsdale, pp. 342–354. Birmingham: Kynoch Press.

Prager, P. R. (1983). *Growth and characterization of AgI polytypes*. *Crystal growth and characterization of polytype structures*, edited by P. Krishna, pp. 451–491. Oxford: Pergamon Press.

Prasad, B. & Lele, S. (1971). *X-ray diffraction from double hexagonal close-packed crystals with stacking faults*. *Acta Cryst.* A**27**, 54–64.

Rai, R. S., Singh, S. R., Dubey, M. & Singh, G. (1986). *Lattice imaging studies on structure and disorder in SiC polytypes*. *Bull. Minéral.* **109**, 509–527.

9.2.1 (*cont.*)

Ramsdell, L. S. (1947). *Studies on silicon carbide. Am. Mineral.* **32**, 64–82.

Sebastian, M. T., Pandey, D. & Krishna, P. (1982). *X-ray diffraction study of the 2H to 3C solid state transformation of vapour grown single crystals of ZnS. Phys. Status Solidi A*, **71**, 633–640.

Steinberger, I. T. (1983). *Polytypism in zinc sulphide. Crystal growth and characterization of polytype structures*, edited by P. Krishna, pp. 7–53. Oxford: Pergamon Press.

Steinberger, I. T., Bordas, J. & Kalman, Z. H. (1977). *Microscopic structure studies of ZnS crystals using synchrotron radiation. Philos. Mag.* **35**, 1257–1267.

Taylor, A. & Jones, R. M. (1960). *The crystal structure and thermal expansion of cubic and hexagonal silicon carbide. Silicon carbide – a high temperature semiconductor*, edited by J. R. O'Connor & J. Smiltens, pp. 147–154. Oxford: Pergamon Press.

Terhell, J. C. J. M. (1983). *Polytypism in the III–VI layer compounds. Crystal growth and characterization of polytype structures*, edited by P. Krishna, pp. 55–109. Oxford: Pergamon Press.

Tokonami, M. & Hosoya, S. (1965). *A systematic method for unravelling a periodic vector set. Acta Cryst.* **18**, 908–916.

Trigunayat, G. C. & Verma, A. R. (1976). *Polytypism and stacking faults in crystals with layer structure. Crystallography and crystal chemistry of materials with layered structures*, edited by F. Levy, pp. 269–340. Dordrecht: Reidel.

Verma, A. R. & Krishna, P. (1966). *Polymorphism and polytypism in crystals*. New York: John Wiley.

Weertman, J. & Weertman, J. R. (1984). *Elementary dislocation theory*. New York: Macmillan.

Wells, A. F. (1945). *Structural inorganic chemistry*. Oxford: Clarendon Press.

Wilson, A. J. C. (1942). *Imperfection in the structure of cobalt. II. Mathematical treatment of proposed structure. Proc. R. Soc. London Ser. A*, **180**, 277–285.

Zhdanov, G. S. (1945). *The numerical symbol of close-packing of spheres and its application in the theory of close-packings. C. R. Dokl. Acad. Sci. URSS,* **48**, 43.

9.2.2

Amelinckx, S. (1986). *High-resolution electron microscopy in materials science. Examining the submicron world*, edited by R. Feder, J. W. McGowan & M. Shinozaki, pp. 71–132. New York: Plenum.

Angel, R. J. (1986). *Polytypes and polytypism. Z. Kristallogr.* **176**, 193–204.

Backhaus, K.-O. & Ďurovič, S. (1984). *Polytypism in micas. I. MDO polytypes and their derivation. Clays Clay Miner.* **32**, 453–464.

Bailey, S. W. (1980). *Structures of layer silicates. Crystal structures of clay minerals and their X-ray identification*, edited by G. M. Brindley & G. Brown, pp. 1–123. London: Mineralogical Society.

Bailey, S. W. (1988*a*) Editor. *Hydrous phyllosilicates* (*Reviews in mineralogy*, Vol. 19). Washington, DC: Mineralogical Society of America.

Bailey, S. W. (1988*b*). *X-ray diffraction indentification of the polytypes of mica, serpentine, and chlorite. Clays Clay Miner.* **36**, 193–213.

Bailey, S. W., Frank-Kamenetskii, V. A., Goldsztaub, S., Kato, A., Pabst, A., Schulz, H., Taylor, H. F. W., Fleischer, M. & Wilson, A. J. C. (1977). *Report of the International Mineralogical Association (IMA)–International Union of Crystallography (IUCr) Joint Committee on Nomenclature. Acta Cryst.* A**33**, 681–684.

Baronnet, A. (1975). *Growth spirals and complex polytypism in micas. I. Polytypic structure generation. Acta Cryst.* A**31**, 345–355.

Baronnet, A. (1986). *Growth spirals and complex polytypism in micas. II. Occurrence frequencies in synthetic species. Bull Minéral.* **109**, 489–508.

Baronnet, A. (1992). *Polytypism and stacking disorder. Reviews in mineralogy*, Vol. 27, pp. 231–288. Washington DC: Mineralogical Society of America.

Baumhauer, H. (1912). *Über die Kristalle des Carborundums. Z. Kristallogr.* **50**, 33–39.

Baumhauer, H. (1915). *Über die verschiedenen Modificationen des Carborundums und die Erscheinung der Polytypie. Z. Kristallogr.* **55**, 249–259.

Belokoneva, E. L. & Timchenko, T. I. (1983). *Polytypic relations in the structures of borates with a general formula* $RAl_3(BO_3)_4$ *(R = Y, Nd, Gd). Kristallografiya,* **28**, 1118–1123. [In Russian.]

Boer, J. L. de, van Smaalen, S., Petříček, V., Dušek, M., Verheijen, M. A. & Meijer, G. (1994). *Hexagonal close-packed C-60. Chem. Phys. Lett.* **219**, 469–472.

Bontchev, R., Darriet, B., Darriet, J., Weill, F., Van Tendeloo, G. & Amelinckx, S. (1993). *New cation deficient perovskite-like oxides in the system* $La_4Ti_3O_{12}$–$LaTiO_3$. *Eur. J. Solid State Inorg. Chem.* **30**, 521–537.

Brindley, G. W. (1980). *Order–disorder in clay mineral stuctures. Crystal structures of clay minerals and their X-ray identification*, edited by G. W. Brindley & G. Brown, pp. 125–195. London: Mineralogical Society.

Burany, X. M. & Northwood, D. O. (1991). *Polytypic structures in close-packed* $Zr(FeCr)_2$ *Laves phases. J. Less-Common Met.* **170**, 27–35.

Carlson, E. H. (1967). *The growth of HgS and* $Hg_3S_2Cl_2$ *single crystals by a vapour phase method. J. Cryst. Growth*, **1**, 271–277.

Chamberland, B. L. (1983). *Crystal structure of the 6H* $BaCrO_3$ *polytype. J. Solid State Chem.* **48**, 318–322.

Císařová, I., Novák, C. & Petříček, V. (1982). *The structure of twinned manganese(III) hydrogenbis(orthophosphite) dihydrate. Acta Cryst.* B**38**, 1687–1689.

Darriet, B., Bovin, J.-O. & Galy, J. (1976). *Un nouveau composé de l'antimoine III:* $VOSb_2O_4$. *Influence stéréochimique de la paire non lié E, relations structurales, mécanismes de la réaction chimique. J. Solid State Chem.* **19**, 205–212.

Dornberger-Schiff, K. (1959). *On the nomenclature of the 80 plane groups in three dimensions. Acta Cryst.* **12**, 173.

Dornberger-Schiff, K. (1964). *Grundzüge einer Theorie von OD-Strukturen aus Schichten. Abh. Dtsch. Akad. Wiss. Berlin. Kl. Chem.* **3**.

Dornberger-Schiff, K. (1966). *Lehrgang über OD-Strukturen*. Berlin: Akademie Verlag.

Dornberger-Schiff, K. (1979). *OD structures – a game and a bit more. Krist. Tech.* **14**, 1027–1045.

Dornberger-Schiff, K. (1982). *Geometrical properties of MDO polytypes and procedures for their derivation. I. General concept and applications to polytype families consisting of OD layers all of the same kind. Acta Cryst.* A**38**, 483–491.

9.2.2 (*cont.*)

Dornberger-Schiff, K., Backhaus, K.-O. & Ďurovič, S. (1982). *Polytypism of micas: OD interpretation, stacking symbols, symmetry relations. Clays Clay Miner.* **30**, 364–374.

Dornberger-Schiff, K. & Ďurovič, S. (1975*a*). *OD interpretation of kaolinite-type structures. I. Symmetry of kaolinite packets and their stacking possibilities. Clays Clay Miner.* **23**, 219–229.

Dornberger-Schiff, K. & Ďurovič, S. (1975*b*). *OD interpretation of kaolinite-type structures. II. The regular polytypes (MDO polytypes) and their derivation. Clays Clay Miner.* **23**, 231–246.

Dornberger-Schiff, K., Ďurovič, S. & Zvyagin, B. B. (1982). *Proposal for general principles for the construction of fully descriptive polytype symbols. Cryst. Res. Technol.* **17**, 1449–1457.

Dornberger-Schiff, K. & Fichtner, K. (1972). *On the symmetry of OD structures consisting of equivalent layers. Krist. Tech.* **7**, 1035–1056.

Dornberger-Schiff, K. & Grell, H. (1982*a*). *Geometrical properties of MDO polytypes and procedures for their derivation. II. OD families containing OD layers of M > 1 kinds and their MDO polytypes. Acta Cryst.* A**38**, 491–498.

Dornberger-Schiff, K. & Grell, H. (1982*b*). *On the notions: crystal, OD crystal and MDO crystal. Kristallografiya*, **27**, 126–133. [In Russian.]

Ďurovič, S. (1968). *The crystal structure of γ-$Hg_3S_2Cl_2$. Acta Cryst.* B**24**, 1661–1670.

Ďurovič, S. (1974*a*). *Notion of 'packets' in the theory of OD structures of M > 1 kinds of layers. Examples: kaolinites and MoS_2. Acta Cryst.* B**30**, 76–78.

Ďurovič, S. (1974*b*). *Die Kristallstruktur des $K_4[Si_8O_{18}]$: Eine desymmetrisierte OD-Struktur. Acta Cryst.* B**30**, 2214–2217.

Ďurovič, S. (1979). *Desymmetrization of OD structures. Krist. Tech.* **14**, 1047–1053.

Ďurovič, S. (1981). *OD-Charakter, Polytypie und Identifikation von Schichtsilikaten. Fortschr. Mineral.* **59**, 191–226.

Ďurovič, S. (1994). *Classification of phyllosilicates according to the symmetry of their octahedral sheets. Ceramics-Silikáty*, **38**, 81–84.

Ďurovič, S. & Dornberger-Schiff, K. (1981). *New fully descriptive polytype symbols for the basic types of clay minerals. 8th Conference on Clay Mineralogy and Petrology, Teplice, Czechoslovakia,* 1979, edited by S. Konta, pp. 19–25. Praha: Charles University.

Ďurovič, S., Dornberger-Schiff, K. & Weiss, Z. (1983). *Chlorite polytypism. I. OD interpretation and polytype symbolism of chlorite structures. Acta Cryst.* B**39**, 547–552.

Ďurovič, S. & Weiss, Z. (1983). *Polytypism of pyrophyllite and talc. Part I. OD interpretation and MDO polytypes. Silikáty*, **27**, 1–18.

Ďurovič, S., Weiss, Z. & Backhaus, K.-O. (1984). *Polytypism of micas. II. Classification and abundance of MDO polytypes. Clays Clay Miner.* **32**, 464–474.

Effenberger, H. (1991). *Structures of hexagonal copper(I) ferrite. Acta Cryst.* C**47**, 2644–2646.

Eggleton, R. A. & Guggenheim, S. (1994). *The use of electron optical methods to determine the crystal structure of a modulated phyllosilicate: parsettensite. Am. Mineral.* **79**, 426–437.

Evans, B. W. & Guggenheim, S. (1988). *Talc, pyrophyllite, and related minerals. Reviews in mineralogy*, Vol. 19, edited by S. W. Bailey, pp. 225–294. Washington, DC: Mineralogical Society of America.

Fichtner, K. (1965). *Zur Existenz von Gruppoiden verschiedener Ordnungsgrade bei OD-Strukturen aus gleichartigen Schichten. Wiss. Z. Tech. Univ. Dresden,* **14**, 1–13.

Fichtner, K. (1977). *Zur Symmetriebeschreibung von OD-Kristallen durch Brandtsche und Ehresmannsche Gruppoide. Beitr. Algebra Geom.* **6**, 71–79.

Fichtner, K. (1979*a*). *On the description of symmetry of OD structures (I). OD groupoid family, parameters, stacking. Krist. Tech.* **14**, 1073–1078.

Fichtner, K. (1979*b*). *On the description of symmetry of OD structures (II). The parameters. Krist. Tech.* **14**, 1453–1461.

Fichtner, K. (1980). *On the description of symmetry of OD structures (III). Short symbols for OD groupoid families. Krist. Tech.* **15**, 295–300.

Fichtner, K. & Grell, H. (1984). *Polytypism, twinning and disorder in 2,2-aziridinedicarboxamide. Acta Cryst.* B**40**, 434–436.

Fichtner-Schmittler, H. (1979). *On some features of X-ray powder patterns of OD structures. Krist. Tech.* **14**, 1079–1088.

Figueiredo, M. O. D. (1979). *Características de empilhamento e modelos condensados das micas e filossilicatos afins*. Lisboa: Junta de Investigacoes Científicas do Ultramar.

Franzini, M. (1969). *The A and B mica layers and the crystal structure of sheet silicates. Contrib. Mineral. Petrol.* **21**, 203–224.

Frueh, A. J. & Gray, N. (1968). *Confirmation and refinement of the structure of $Hg_3S_2Cl_2$. Acta Cryst.* B**24**, 156.

Gard, J. A. & Taylor, H. F. W. (1960). *The crystal structure of foshagite. Acta Cryst.* **13**, 785–793.

Grell, H. (1984). *How to choose OD layers. Acta Cryst.* A**40**, 95–99.

Grell, H. & Dornberger-Schiff, K. (1982). *Symbols for OD groupoid families referring to OD structures (polytypes) consisting of more than one kind of layer. Acta Cryst.* A**38**, 49–54.

Guinier, A., Bokij, G. B., Boll-Dornberger, K., Cowley, J. M., Ďurovič, S., Jagodzinski, H., Krishna, P., de Wolff, P. M., Zvyagin, B. B., Cox, D. E., Goodman, P., Hahn, Th., Kuchitsu, K. & Abrahams, S. C. (1984). *Nomenclature of polytype structures. Report of the International Union of Crysallography Ad-Hoc Committee on the Nomenclature of Disordered, Modulated and Polytype Structures. Acta Cryst.* A**40**, 399–404.

Hamid, S. A. (1981). *The crystal structure of the 11 Å natural tobermorite $Ca_{2.25}[Si_3O_{7.5}(OH)_{1.5}]\cdot 1H_2O$. Z. Kristallogr.* **154**, 189–198.

Heinrich, A. R., Eggleton, R. A. & Guggenheim, S. (1994). *Structure and polytypism of bementite, a modulated layer silicate. Am. Mineral.* **79**, 91–106.

Iijima, S. (1982). *High-resolution electron microscopy of mcGillite. II. Polytypism and disorder. Acta Cryst.* A**38**, 695–702.

Ingrin, J. (1993). *TEM imaging of polytypism in pseudowollastonite. Phys. Chem. Miner.* **20**, 56–62.

Ito, T., Sadanaga, R., Takéuchi, Y. & Tokonami, M. (1969). *The existence of partial mirrors in wollastonite. Proc. Jpn Acad.* **45**, 913-918.

Jagner, S. (1985). *On the origin of the order–disorder structures (polytypes) of some transition metal hexacyano complexes. Acta Chem. Scand.* **139**, 717–724.

Jagodzinski, H. (1964). *Allgemeine Gesichtspunkte für die Deutung diffuser Interferenzen von fehlgeordneten Kristallen. Advances in structure research by diffraction methods*, Vol. I, edited by R. Brill, pp. 167–198. Braunschweig: Vieweg, and New York/London: Interscience.

9.2.2 (*cont.*)

Jarchow, O. & Schmalle, H. W. (1985). *Fehlordnung, Polytypie und Struktur von Primetin: 5,8-Dihydroxy-2-phenylchromen-4-on*. *Z. Kristallogr.* **173**, 225–236.

Kaneko, F., Sakashita, H., Kobayashi, M., Kitagawa, Y., Matsuura, U. & Suzuki, M. (1994). *Double-layered polytypic structure of the E form of octadecanoic acid, $C_{18}H_{36}O_2$*. *Acta Cryst.* C**50**, 247–250.

Kowalski, M. (1985). *Polytypic structures of chromium iron [$(Cr,Fe)_7C_3$] carbides*. *J. Appl. Cryst.* **18**, 430–435.

Kuban, R.-J. (1985). *Polytypes of the system $Fe_{1-x}S$*. *Cryst. Res. Technol.* **20**, 1649–1656.

Kutschabsky, L., Kretschmer, R.-G., Schrauber, H., Dathe, W. & Schneider, G. (1986). *Structure of the OD disordered 2-hydroxy-4-methoxy-2H-1,4-benzoxazin-3-one, $C_9H_9NO_4$*. *Cryst. Res. Technol.* **21**, 1521–1529.

McLarnan, T. J. (1981*a*). *Mathematic tools for counting polytypes*. *Z. Kristallogr.* **155**, 227–245.

McLarnan, T. J. (1981*b*). *The number of polytypes of sheet silicates*. *Z. Kristallogr.* **155**, 247–268.

McLarnan, T. J. (1981*c*). *The number of polytypes in close packings and related structures*. *Z. Kristallogr.* **155**, 269–291.

Makovický, E., Leonardsen, E. & Moelo, Y. (1994). *The crystallography of lengenbachite, a mineral with the non-commensurate layer structure*. *N. Jahrb. Mineral. Abh.* **166**, 169–191.

Mellini, M., Merlino, S. & Pasero, M. (1986). *X-ray and HRTEM structure analysis of orientite*. *Am. Mineral.* **71**, 176–187.

Merlino, S., Orlandi, P., Perchiazzi, N., Basso, R. & Palenzona, A. (1989). *Polytypism in stibivanite*. *Can. Mineral.* **27**, 625–632.

Merlino, S., Pasero, M., Artioli, G. & Khomyakov, A. P. (1994). *Penkvilskite, a new kind of silicate structure – OD character, X-ray single-crystal (1M), and powder Rietveld (2O) refinements of 2 MDO polytypes*. *Am. Mineral* **79**, 1185–1193.

Merlino, S., Pasero, M. & Perchiazzi, N. (1993). *Crystal structure of paralaurionite and its OD relationship with laurionite*. *Mineral. Mag.* **57**, 323–328.

Merlino, S., Pasero, M. & Perchiazzi, N. (1994). *Fiedlerite – revised chemical formula ($Pb_3Cl_4F(OH)\cdot H_2O$), OD description and crystal-structure refinement of the 2 MDO polytypes*. *Mineral Mag.* **58**, 69–78.

Mogami, K., Nomura, K., Miyamoto, M., Takeda, H. & Sadanaga, R. (1978). *On the number of distinct polytypes of mica and SiC with a prime layer-number*. *Can. Mineral.* **16**, 427–435.

Müller, U. & Conradi, E. (1986). *Fehlordnung bei Verbindungen MX_3 mit Schichtenstruktur. I. Berechnung des Intensitätsverlaufs auf den Streifen der diffusen Röntgenstreuung*. *Z. Kristallogr.* **176**, 233–261.

Nikolin, B. I. (1984). *Multi-layer structures and polytypism in metallic alloys*. *Kiev: Naukova dumka*. [In Russian.]

Nikolin, B. I., Babkevich, A. Yu., Izdkovskaya, T. V. & Petrova, S. N. (1993). *Effect of heat-treatment on the crystalline structure of martensite in iron-doped, nickel-doped, manganese-doped and silicon-doped Co–W and Co–Mo alloys*. *Acta Metall.* **41**, 513–515.

Pasero, M. & Reinecke, T. (1991). *Crystal-chemistry, HRTEM analysis and polytypic behavior of ardennite*. *Eur. J. Mineral.* **3**, 819–830.

Pauling, L. (1930*a*). *Structure of micas and related minerals*. *Proc. Natl Acad. Sci. USA*, **16**, 123–129.

Pauling, L. (1930*b*). *Structure of the chlorites*. *Proc. Natl Acad. Sci. USA*, **16**, 578–582.

Phelps, A. W., Howard, W. & Smith, D. K. (1993). *Space groups of the diamond polytypes*. *J. Mater. Res.* **8**, 2835–2839.

Pring, A. & Graeser, S. (1994). *Polytypism in baumhauerite*. *Am. Mineral.* **79**, 302–307.

Radoslovich, E. W. (1961). *Surface symmetry and cell dimensions of layer-lattice silicates*. *Nature (London)*, **191**, 67–68.

Reck, G. & Dietz, G. (1986). *The order–disorder structure of carbamazepine dihydrate: 5H-dibenz[b,f]azepine-5-carboxamide dihydrate, $C_{15}H_{12}N_2O\cdot 2H_2O$*. *Cryst. Res. Technol.* **21**, 1463–1468.

Reck, G., Dietz, G., Laban, G., Günther, W., Bannier, G. & Höhne, E. (1988). *X-ray studies on piroxicam modifications*. *Pharmazie*, **43**, 477–481.

Ross, M., Takeda, H. & Wones, D. R. (1966). *Mica polytypes: systematic description and identification*. *Science*, **151**, 191–193.

Schwarz, W. & Blaschko, O. (1990). *Polytype structures of lithium at low-temperatures*. *Phys. Rev. Lett.* **65**, 3144–3147.

Sedlacek, P., Kuban, R.-J. & Backhaus, K.-O. (1987). *Structure determination of polytypes*. *Cryst. Res. Technol.* **22**, 793–798 (I), 923–928 (II).

Smaalen, S. van & de Boer, J. L. (1992). *Structure of polytype of the inorganic misfit-layer compound $(PbS)1.18TiS_2$*. *Phys. Rev B*, **46**, 2750–2757.

Smith, J. V. & Yoder, H. S. (1956). *Experimental and theoretical studies of the mica polymorphs*. *Mineral. Mag.* **31**, 209–235.

Sorokin, N. D., Tairov, Yu. M., Tsvetkov, V. F. & Chernov, M. A. (1982). *The laws governing the changes of some properties of different silicon carbide polytypes*. *Dokl. Akad. Nauk SSSR,* **262**, 1380–1383. [In Russian]. See also *Kristallografiya*, **28**, 910–914.

Szymański, J. T. (1980). *A redetermination of the structure of Sb_2VO_5, stibivanite, a new mineral*. *Can. Mineral.* **18**, 333–337.

Takéuchi, Y., Ozawa, T. & Takahata, T. (1983). *The pyrosmalite group of minerals. III. Derivation of polytypes*. *Can. Mineral.* **21**, 19–27.

Taxer, K. (1992). *Order–disorder and polymorphism of the compound with the composition of scholzite, $CaZn_2[PO_4]_2\cdot 2H_2O$*. *Z. Kristallogr.* **198**, 239–255.

Thompson, J. B (1981). *Polytypism in complex crystals: contrasts between mica and classical polytypes. Structure and bonding in crystals II*, edited by M. O'Keefe & A. Navrotsky, pp. 168–196. New York/London/Toronto/Sydney/San Francisco: Academic Press.

Tomaszewski, P. E. (1992). *Polytypism of α-$LiNH_4SO_4$ crystals*. *Solid State Commun.* **81**, 333–335.

Tsvetkov, V. F. (1982). *Problems and prospects of growing large silicon carbide single crystals*. *Izv. Leningr. Elektrotekh. Inst.* **302**, 14–19. [In Russian.]

Verma, A. J. & Krishna, P. (1966). *Polymorphism and polytypism in crystals*. New York: John Wiley.

Weiss, Z. & Ďurovič, S. (1980). *OD interpretation of Mg-vermiculite. Symbolism and X-ray identification of its polytypes*. *Acta Cryst.* A**36**, 633–640.

Weiss, Z. & Ďurovič, S. (1983). *Chlorite polytypism. II. Classification and X-ray identification of trioctahedral polytypes*. *Acta Cryst.* B**39**, 552–557.

Weiss, Z. & Ďurovič, S. (1985*a*). *Polytypism of pyrophyllite and talc. Part II. Classification and X-ray identification of MDO polytypes*. *Silikáty,* **28**, 289–309.

9.2.2 (*cont.*)

Weiss, Z. & Ďurovič, S. (1985*b*). *A unified classification and X-ray identification of polytypes of 2:1 phyllosilicates. 5th Meeting of the European Clay Groups, Prague*, 1983, edited by J. Konta, pp. 579–584. Praha: Charles University.

Weiss, Z. & Wiewióra, A. (1986). *Polytypism in micas. III. X-ray diffraction identification. Clays Clay Miner.* **34**, 53–68.

Wennemer, M. & Thompson, A. B. (1984). *Tridymite polymorphs and polytypes. Schweiz. Mineral. Petrogr. Mitt.* **64**, 335–353.

White, T. J., Segall, R. L., Hutchison, J. L. & Barry, J. C. (1984). *Polytypic behaviour of zirconolite. Proc. R. Soc. London Ser. A*, **392**, 343–358.

Yamanaka, T. & Mori, H. (1981). *The crystal structure and polytypes of α-$CaSiO_3$ (pseudowollastonite). Acta Cryst.* B**37**, 1010–1017.

Zhukhlistov, A. P., Zvyagin, B. B. & Pavlishin, V. I. (1990). *The polytype 4M of the Ti-biotite displayed on an oblique-texture electron-diffraction pattern. Kristallografiya,* **35**, 406–413. [In Russian.]

Zoltai, T. & Stout, J. H. (1985). *Mineralogy: concepts and principles*. Minneapolis, Minnesota: Burgess.

Zorkii, P. M. & Nesterova, Ya. M. (1993). *Interlayered polytypism in organic crystals. Zh. Fiz. Khim.* **67**, 217–220. [In Russian.]

Zvyagin, B. B. (1964). *Electron diffraction analysis of clay minerals*. Moskva: Nauka. [In Russian.]

Zvyagin, B. B. (1967). *Electron diffraction analysis of clay minerals*. New York: Plenum.

Zvyagin, B. B. (1988). *Polytypism in crystal structures. Comput. Math. Appl.* **16**, 569–591.

Zvyagin, B. B. & Fichtner, K. (1986). *Geometrical conditions for the formation of polytypes with a supercell in the basis plane. Bull. Minéral.* **109**, 45–47.

Zvyagin, B. B., Vrublevskaya, Z. V., Zhoukhlistov, A. P., Sidorenko, O. V., Soboleva, S. V. & Fedotov, A. F. (1979). *High-voltage electron diffraction in the investigation of layered minerals*. Moskva: Nauka [In Russian.]

9.3

Brunner, G. O. & Schwarzenbach, D. (1971). *Zur Abgrenzung der Koordinationsphäre und Ermittlung det Koordinationszahl in Kristallstrukturen. Z. Kristallogr.* **133**, 127–133.

Daams, J. L. C. (1995). *Atomic environments in some related intermetallic structure types. Intermetallic compounds, principles and practice*, edited by J. H. Westbrook & R. L. Fleischer, Vol. 1, pp. 363–383. New York: John Wiley.

Daams, J. L. C. & Villars, P. (1993). *Atomic-environment classification of the rhombohedral ''intermetallic'' structure types. J. Alloys Compd.* **197**, 243–269.

Daams, J. L. C. & Villars, P. (1994). *Atomic-environment classification of the hexagonal ''intermetallic'' structure types. J. Alloys Compd.* **215**, 1–34.

Daams, J. L. C. & Villars, P. (1997). *Atomic enironment classification of the tetragonal ''intermetallic'' structure types. J. Alloys Compd.* **252**, 110–142.

Daams, J. L. C., Villars, P. & van Vucht, J. H. N. (1991). *Atlas of crystal structure types for intermetallic phases*. Materials Park, OH: ASM International.

Daams, J. L. C., Villars, P. & van Vucht, J. H. N. (1992). *Atomic-environment classification of the cubic ''intermetallic'' structure types. J. Alloys Compd.* **182**, 1–33.

Kordes, E. (1939*a*). *Die Ermittlung von Atomabständen aus der Lichtbrechnung. I. Mitteilung. Über eine einfache Beziehung zwischen Ionenrefraktion, Ionenradius und Ordnungszahl der Elemente. Z. Phys. Chem. B*, **44**, 249–260.

Kordes, E. (1939*b*) *Die Ermittlung von Atomabständen aus der Lichtbrechnung. II. Mitteilung. Z. Phys. Chem. B*, **44**, 327–343.

Kordes, E. (1940). *Ionenradien und periodisches System. II. Mitteilung. Berechnung der Ionenradien mit Hilfe atomphysicher Grössen. Z. Phys. Chem.* **48**, 91–107.

Kordes, E. (1960). *Direkte Berechnung der Ionenradien allein aus den Ionen-abständen. Naturwissenschaften*, **47**, 463.

Pauling, L. (1947). *The nature of the interatomic forces in metals. II. Atomic radii and interatomic distances in metals. J. Am. Chem. Soc.* **69**, 542–553.

Pearson, W. B. (1979). *The stability of metallic phases and structures: phases with the AlB_2 and related structures. Proc. R. Soc. London Ser. A*, **365**, 523–535.

Rodgers, J. R. & Villars, P. (1988). *Computer evaluation of crystallographic data*. In *Proceedings of the 11th International CODATA Conference, Karlsruhe, FRG*, edited by P. S. Glaeser. New York: Hemisphere Publishing Corp.

Samsonov, G. V. (1968). Editor. *Handbook of physicochemical properties of elements*, p. 98. New York/Washington: IFI/Plenum Data Corporation.

Teatum, E. T., Gschneider, K. Jr & Waber, J. T. (1960). *Compilation of calculated data useful in predicting metallurgical behaviour of the elements in binary alloy systems*. USAEC Report LA–2345, 225 pp. Washington, DC: United States Atomic Energy Commission.

Teatum, E. T., Gschneider, K. Jr & Waber, J. T. (1968). *Compilation of calculated data useful in predicting metallurgical behaviour of the elements in binary alloy systems*. USAEC Report LA–4003, 206 pp. [Supercedes Report LA-2345 (1960).] Washington, DC: United States Atomic Energy Commission.

Villars, P. & Calvert, L. D. (1991). *Pearson's handbook of crystallographic data for intermetallic phases*, 2nd ed. Materials Park, OH: ASM International.

Villars, P. & Girgis, K. (1982). *Regelmäßigkeiten in binären intermetallischen Verbindungen. Z. Metallkd.* **73**, 455–462.

9.4

Bergerhoff, G. & Brown, I. D. (1987). *Inorganic crystal structure database*. In *Crystallographic databases*, edited by F. H. Allen, G. Bergerhoff & R. Sievers, pp. 77–95. Bonn/Cambridge/Chester: International Union of Crystallography.

International Tables for X-ray Crystallography (1962). Vol. III, pp. 257–274. Birmingham: Kynoch Press.

Sievers, R. & Hundt, R. (1987). *Crystallographic information system CRYSTIN*. In *Crystallographic databases*, edited by F. H. Allen, G. Bergerhoff & R. Sievers, pp. 210–221. Bonn/Cambridge/Chester: International Union of Crystallography.

9.5

Allen, F. H., Bellard, S., Brice, M. D., Cartwright, B. A., Doubleday, A., Higgs, H., Hummelink, T., Hummelink-Peters, B. G., Kennard, O., Motherwell, W. D. S., Rodgers, J. R. & Watson, D. G. (1979). *The Cambridge Crystallographic Data Centre: computer-based search, retrieval, analysis and display of information. Acta Cryst.* B**35**, 2331–2339.